

Scale-Dependent Processes and Runout in Bidisperse Granular Flows: Insights From Laboratory Experiments and Implications for Rock/Debris Avalanches



Key Points:

- For bidispersity to enhance the runout of analog granular avalanches, a collisional regime and particle segregation are required
- Dynamic scaling suggests that processes and flow regimes reducing apparent friction in small analog experiments are scale-dependent
- Lack of signature of agitation and size segregation reported in large field-scale avalanche sedimentology suggests dissimilar processes

Supporting Information:

Supporting Information may be found in the online version of this article.

Correspondence to:

S. Makris,
smakr@bgs.ac.uk




Citation:

Makris, S., Manzella, I., & Sgarabotto, A. (2024). Scale-dependent processes and runout in bidisperse granular flows: Insights from laboratory experiments and implications for rock/debris avalanches. *Journal of Geophysical Research: Earth Surface*, 129, e2023JF007469. <https://doi.org/10.1029/2023JF007469>

Received 1 OCT 2023
Accepted 23 JUL 2024

Author Contributions:

Conceptualization: S. Makris, I. Manzella
Formal analysis: S. Makris
Investigation: S. Makris, A. Sgarabotto
Methodology: S. Makris, I. Manzella
Supervision: I. Manzella
Writing – original draft: S. Makris
Writing – review & editing: S. Makris, I. Manzella, A. Sgarabotto

S. Makris^{1,2} , I. Manzella^{1,3} , and A. Sgarabotto^{1,4} 

¹School of Geography, Earth and Environmental Science, University of Plymouth, Plymouth, UK, ²British Geological Survey (BGS), Edinburgh, UK, ³Department of Applied Earth Sciences, Faculty of Geo-Information Science and Earth Observation (ITC), University of Twente, Enschede, The Netherlands, ⁴Now at School of Engineering, University of Birmingham, Birmingham, UK

Abstract The bidispersity observed in the particle-size distribution of rock avalanches and volcanic debris avalanches (rock/debris avalanches) has been proposed as a factor contributing to their long runout. This has been supported by small-scale analog experimental studies, which observe that a small proportion of fine particles mixed with coarser particles enhances granular avalanche runout. However, the mechanisms enabling this phenomenon and their resemblance to rock/debris avalanches have not been directly evaluated. Here, binary mixture granular avalanche experiments are employed to constrain the processes and conditions under which bidispersity enhances the runout of granular avalanches in experiments. Structure-from-motion photogrammetry is used to measure center of mass displacement and assess energy dissipation. Subsequently, this study evaluates the dynamic scaling and flow regimes in the lab and field to assess whether the runout-enhancing mechanism is applicable to rock/debris avalanches. In small-scale experiments, the granular mass propagates under a collisional regime, enabling kinetic sieving and size segregation. Fine particles migrate to the base where they reduce frictional areas between coarse particles and the substrate and encourage rolling. The reduced energy dissipation increases the kinetic energy conversion and avalanche mobility. However, rock/debris avalanches are unlikely to acquire a purely collisional regime; instead, they propagate under a frictional regime. The size segregation which is essential for the process observed at the lab-scale is prohibited by the frictional regime, as evident by the sedimentology of rock/debris avalanche deposits. The proposal of bidispersity as a runout-enhancing mechanism overlooks that scale-dependent behaviors of natural events are often omitted in small-scale experiments.

Plain Language Summary Large landslides such as rock avalanches and volcanic debris avalanches flow unexpectedly long distances before stopping. The mechanisms generating this phenomenon remain unknown. The fact that they contain large proportions of finer and coarser particles (with relatively smaller quantities of the sizes between them) has been suggested by experiments to be a potential factor for the long distances they cover. In this work, we have carried out experiments to examine the processes enabling this event at the scale of lab experiments in order to assess their potential in real events. We found that this phenomenon is caused by fine particles percolating to the base of the flow. There, they reduce the surface of the coarse particles, which are in contact with the substrate, and also encourage the rolling of the coarser particles. This reduces frictional energy loss, and conserves more energy, which contributes to the flow, leading to longer distances. However, the conditions which allow these processes and the percolation of the fine particles to the base are scale-dependent and are not applicable to large-scale events. When planning granular flow experiments or interpreting their findings, scaling is important to ensure similarity between the experimental conditions and the physical processes targeted.

1. Introduction

Rock avalanches are rapid mass movements that evolve from the detachment of a rock mass which partially disaggregates into a granular flow during propagation (Hungry et al., 2014; Scott et al., 2001). Volcanic debris avalanches are the equivalent mass flow of the volcanic environment, mobilizing volcanic material after the collapse of unstable volcanic flanks (Roverato et al., 2021; Ui, 1983). Both mass flow types (subsequently rock/debris avalanches collectively) achieve much greater horizontal runout distance compared to their fall height (Davies, 1982; Hungry, 2002; Legros, 2002), far greater than predicted by simple frictional models of a coherent

© 2024. The Author(s).

This is an open access article under the terms of the [Creative Commons Attribution License](https://creativecommons.org/licenses/by/4.0/), which permits use, distribution and reproduction in any medium, provided the original work is properly cited.

sliding mass (Rait & Bowman, 2016). This study is focused on the processes that have been observed and reported in large rock avalanches of $>10^5$ – 10^6 m³ (Dufresne et al., 2021; Legros, 2002; McSaveney & Davies, 1999) and debris avalanches of >0.1 km³ (Bernard et al., 2021). This distinction is made to clarify the focus of this study on large scale events, with a matrix facies component and undisaggregated block facies component, and exclude small landslide and rockfall type events. This size distinction is often made in the literature (e.g., McSaveney & Davies, 1999), when examining mass flows with the lowest apparent friction coefficients, and therefore, longer runouts (e.g., Johnson et al., 2016; Legros, 2002). To explain the long runout, a mechanism that accounts for the apparent decrease in the effective friction coefficient is required. Despite numerous proposed theories, none are consistent with field observations, leaving the issue controversial and unresolved, necessitating an evaluation of theoretical models against field data (Banton et al., 2009; Cabrera & Estrada, 2021; Davies & McSaveney, 2012; Perinotto et al., 2015; Pollet & Schneider, 2004).

Propagating rock/debris avalanches are believed to behave as dense granular flows where particle interactions are the most important energy dissipation process, and fluid effects are negligible (Campbell, 1990; Davies & McSaveney, 1999; Legros, 2002; Makris et al., 2020; Reubi & Hernandez, 2000; Schneider & Fisher, 1998; Voight et al., 1983). The flow is controlled by particle interactions, internal and basal friction coefficients, and interactions with boundaries and path geometry (Denlinger & Iverson, 2001; Iverson, 1997; Roche et al., 2021). Particle interactions generate momentum transfer and dissipation as well as energy dissipated in other forms such as friction and acoustic energy generation in a process referred to as the granular effect (Hu et al., 2020). The magnitude of the kinetic energy exchange is measured as the granular temperature (Campbell, 1990; Iverson, 1997; Sanvitale & Bowman, 2016). The granular effect is a function of the particle shape, density, size, hardness and roughness (Bartali et al., 2015; Polanía et al., 2023) and the flow processes controlling their interactions. Therefore, particle-size distribution properties can potentially affect propagation dynamics. The interaction of particles with different sizes has been proposed as a potential factor for the long runouts of rock/debris avalanches.

Rock/debris avalanche deposits are composed of angular/subangular clasts spanning a size range from fine particles smaller than 1 μ m up to tens of meters (e.g., Makris, Roverato, Dávila-harris, et al., 2023; McSaveney & Davies, 2002; Roche et al., 2006; Voight, 1978). Heterogeneity can arise from the source material or fragmentation and comminution during propagation (Crosta et al., 2007; Davies & McSaveney, 2012; De Blasio & Crosta, 2014; Dufresne & Dunning, 2017; Knapp & Krautblatter, 2020; McSaveney & Davies, 2002). Furthermore, rock/debris avalanche deposits are characterized by bidisperse to polydisperse particle-size distributions (e.g., Bernard et al., 2017; Glicken, 1996; Pollet & Schneider, 2004; Scott et al., 1995; Vallance, 2000; Vallance & Iverson, 2015). Recent studies have supported that a bidisperse particle-size distribution is capable of providing a more energy-efficient shear accommodation arrangement and reducing frictional losses at the base of rock/debris avalanches. Studies including Linares-Guerrero et al. (2007), Yang et al. (2015), and more recently Bartali et al. (2020), Hu et al. (2021), and Duan et al. (2022) propose bidispersity as a contributing factor to the long runouts observed in the field. Nonetheless, other studies including the recent triaxial shear test experiments of Polanía et al. (2023 and references therein) suggest that bidispersity or particle-size distribution (Ahmed et al., 2023) do not affect the shear strength or internal friction of granular mixtures. Therefore, the potential effect of bidispersity and the conditions under which this property can affect the dynamics of granular flows remain unclear. This study constrains the processes that have led to the observation of enhanced runouts and evaluates them as potential factors contributing to the long runouts of rock/debris avalanches.

Column collapse and granular avalanche experiments (e.g., Degaetano et al., 2013; Goujon et al., 2007; Hu et al., 2020; Li et al., 2021; Moro et al., 2010; Phillips et al., 2006; Yang et al., 2015) as well as numerical models (e.g., Cabrera & Estrada, 2021; Hu et al., 2021; Linares-Guerrero et al., 2007), have been employed to study the behavior of granular mixtures composed of more than one particle size. Analog experiments such as those of Goujon et al. (2007), Yang et al. (2015), Bartali et al. (2020), Hu et al. (2020), and Duan et al. (2022) evaluate the behavior of granular avalanches (i.e., not column collapse) composed of combinations of two size species of particles (binary and bidisperse). Such studies have observed that the addition of a small proportion of finer particles to a granular mixture generates enhanced runouts (e.g., Duan et al., 2022; Moro et al., 2010; Roche et al., 2006; Yang et al., 2015). Although empirical relationships between single parameters under bidispersity have been established, limited attention has been given to the particle interaction mechanisms affecting energy dissipation and mobility (Li et al., 2021). Even less consideration has been given to the applicability of the relevant granular effects on large-scale geophysical flows, which has not been directly addressed so far.

Therefore, the objectives of this study are as follows: (a). Identify the mechanisms responsible for the long runouts observed in the analog bidisperse experiments, (b). Evaluate whether these factors are likely to be factors for the long runouts of large rock/debris avalanches, and (c). Examine the scaling requirements for the planning and interpreting analog granular flow experiments that can explore the dynamics of rock/debris avalanches.

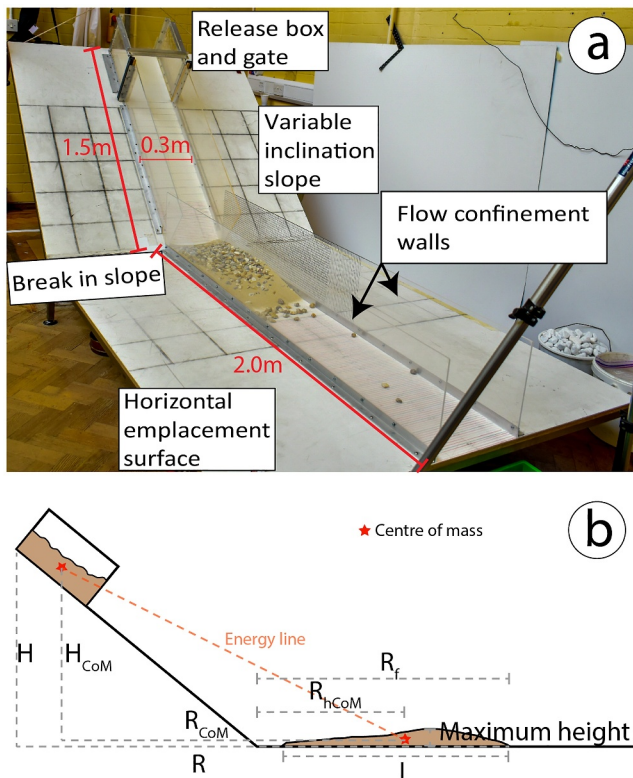
This work evaluates the impact of bidisperse particle-size distributions on the propagation and energy dissipation in small-scale granular avalanche experiments using different binary particle size mixtures. It also examines the combined effects of volume, inclination, and particle size ratio to better understand the influence of bimodality on the granular effect. This study analyses the center of mass and frontal velocity to understand the mechanisms driving granular avalanche runout. By examining these dynamics, this study constrains the processes under which bidispersity enhances mobility. Subsequently, the potential of these processes as a factor for the enhanced mobility of rock/debris avalanches and other natural geophysical flows is evaluated.

2. Bidispersity and Mobility—Background

Lab-scale analog experiments suggest that granular avalanches containing more than one particle size (i.e., bidisperse or polydisperse) diverge in their macroscale properties from avalanches with monodisperse particle-size distributions (e.g., Goujon et al., 2007; Phillips et al., 2006; Reubi et al., 2005; Roche et al., 2006; Yang et al., 2015). One of the main differences commonly observed is that the addition of a small fraction of fine particles to a mass composed of coarser particles results in increased velocity and runout of the center of mass and the front of avalanches (e.g., Degaetano et al., 2013; Phillips et al., 2006; Roche et al., 2006; Yang et al., 2015). The proportion of fine particles to the total mass is denoted as ψ . Analog experiments suggest that maximum frontal runout is achieved at a critical ψ value (ψ_{CRF}) (e.g., Bartali et al., 2020; Hu et al., 2020; Kokelaar et al., 2014; Moro et al., 2010; Phillips et al., 2006). The ψ_{CRF} has been suggested under the bidisperse experimental conditions of Phillips et al. (2006), Roche et al. (2006), and Hu et al. (2020) to be equal to 0.30. In the experiments of Moro et al. (2010), ψ_{CRF} was equal to 0.25; for Degaetano et al. (2013) 0.50, and Duan et al. (2022) 0.05. The ψ_{CRF} was found to be variable according to the particle size composition and other experimental conditions such as slope inclination of the flow path by other studies (Goujon et al., 2007; Yang et al., 2015). A comparison of the experimental conditions of these studies is presented in Table S1 in Supporting Information S2.

Investigation of the mechanisms facilitating the increased runout effect in these experiments has led to a number of observations, resulting in a theoretical conceptual model based on their interpretation. The study of Phillips et al. (2006) reveals that in small-scale avalanches, fine particles migrate rapidly to the base. Once at the base, fine particles have been suggested to reduce the frictional areas between the coarse particles and the substrate by occupying the area between them and acting as “ball-bearings” supporting the coarser particles over the substrate (Linares-Guerrero et al., 2007; Oda & Kazama, 1998; Roche et al., 2006). They simultaneously act as “rollers” to encourage rolling as opposed to frictional sliding (Hu et al., 2021; Phillips et al., 2006). This process interpretation is based on numerical modeling of binary size distribution granular avalanches where rotational motion is enhanced at their base (Hu et al., 2021; Linares-Guerrero et al., 2007). In this case, rolling would reduce the friction coefficient at the base of the flow as it is less expensive in terms of energy dissipation, and increases the efficiency of kinetic energy transfer (Hu et al., 2020, 2021; Phillips et al., 2006). In effect, a basal layer of fine particles is suggested to reduce the friction coefficient between the granular body and the propagation surface (Lai et al., 2017), inhibiting frictional energy losses.

However, this idealized behavior has to be linked to the scale and processes of natural events. One hypothesis, supported by the studies of Linares-Guerrero et al. (2007), Yang et al. (2015), Lai et al. (2017), Hu et al. (2021), and Duan et al. (2022), suggests that in rock/debris avalanches, fine particles migrate and lubricate the base, in a process equivalent to the described lab experiments. It is suggested that fine particles enable rolling instead of sliding, locally accommodating shear stress, with the rest of the mass carried sliding on the basal layer, without experiencing agitation, shear stress and energy losses (Hu et al., 2021). However, recent studies show that the shear strength and residual friction angles of sufficiently large granular systems are independent of particle-size distributions (e.g., Ahmed et al., 2023; Cabrera & Estrada, 2021; Polanía et al., 2023). Therefore, further evaluation is required to understand the mechanisms by which bidispersity could contribute to the enhanced mobility observed in lab experiments and natural granular flows.



3. Methodology

3.1. Experimental Setup and Measuring Systems

The experimental setup is comprised of a 1.5 m long inclined plane and a 2.0 m horizontal depositional surface (Figure 1a). The substrate of the flows is relatively smooth but does not result in sliding of the material and plug flow (Roche et al., 2021). The material is laterally confined during propagation by transparent plastic walls, limiting its width to 0.3 m. The smoothness of the walls and the fact that the ratio between the mean particle diameter and the flow width is $<1/20$ ensure that boundary effects are negligible in the majority of the experiments (Ahmadipur et al., 2019; Jiang & Zhao, 2015; Schilirò et al., 2019; Valentino et al., 2008). The ratio is $>1/20$ (1/15.62) for the coarsest gravel species, which might introduce boundary effects in portions of the flow composed entirely of coarse gravel. Confined avalanches do not exhibit the flow and depositional morphologies of unconfined. Nonetheless, the purpose was the detailed examination of the effect of individual processes and not the recreation of deposit geometry. The confinement did not permit lateral spreading; however, it is assumed that there is no significant effect on the flow dynamics in the flow direction (Thompson et al., 2009—pp246). The inclination of the inclined plane was varied between 35°, 40° and 45°, altering the geometry of the slope-break between the inclined and horizontal surfaces.

Prior to release, the material was held in a release box with a sluice gate removable by sliding upwards. Rapid removal of the gate initiates the flow of material on the inclined plane. After propagating down the incline, the material interacted with the slope-break and subsequently propagated on the horizontal surface. The final deposit was formed when all material became immobile. Propagation is defined as the flow of the material on the inclined and horizontal planes. The final deceleration and deposition are defined as the emplacement stage.

Measurements of the geometry of the material prior to release were made manually and photographs were taken so that the location of the pre-release center of mass of the material in the release box could be calculated.

Manual measurements were taken for the frontal runout (R_f), the length of the deposit (L) and the maximum height of the final deposit (Figure 1b). R_f is defined as the distance traveled by the most distal position on the horizontal plane from the slope-break, where particles are still in contact with the main deposit body. However, for confirmation and higher accuracy measurements, an oblique photogrammetry survey was conducted, as in Li et al. (2021). Photographs of the final deposit were processed using the commercially available software *Agisoft Metashape* to generate a 3D model. A digital elevation model (Figure S1 in Supporting Information S2) allowed calculating the average deposit thickness, the location of the center of mass, the length of the deposit L , and R_f .

Two high-definition cameras recorded the avalanches, one frontal and one lateral (as illustrated in Figure S2 of the Supporting Information S2). The lateral camera view (25 fps, HDV 1,440 × 1,080) was used to observe the interaction of the avalanche with the slope-break. The frontal velocity (V_f) was obtained through the analysis of 50 fps (FHD 1,920 × 1,088) footage from the frontal camera. The location of the front of the flow at each frame was manually located, and the displacement between frame intervals was calculated. A moving average is used in the presented time series with a period of three frames to smooth out short-term fluctuations and highlight longer-lasting trends. Only one of the runs is illustrated in subsequent figures for clarity of illustration. The repeatability of the experiments was ensured by confirming with a minimum of three repetitions.

H/R (often H/L in the literature) is the ratio between the fall height from the highest point of the material in the box to the horizontal plane (H) and the horizontal runout of the front of the avalanche (R —see Figure 1). This ratio is used as a measure of avalanche mobility in landslide literature (initially by Heim (1932)). Although it is often calculated as the distance between the furthest location of the scarp and the toe of the deposit, in this study it is also calculated for the height fallen (H_{CoM}) and horizontal displacement (R_{CoM}) of the center of mass, as H_{CoM}/R_{CoM}

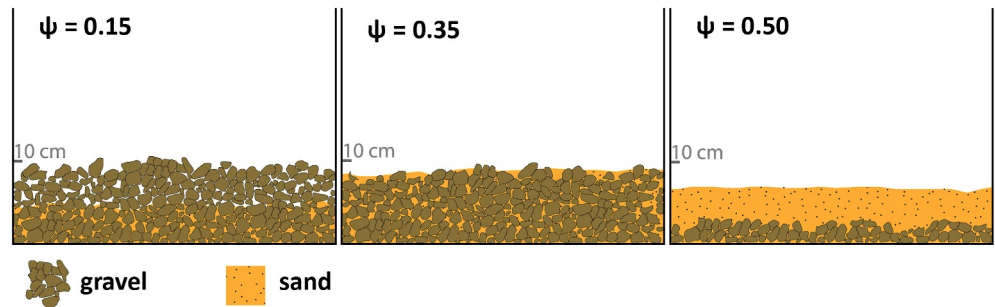


Figure 2. Schematic representation of the pre-release arrangement of material in the release box. Note the difference in volume at different size combinations (although weight is equal) as well as the pore spaces between coarse particles at low fractions of fine particles (i.e. low ψ).

(also referred to as the gradient of the energy line) (Legros, 2002). The displacement of the center of mass is a better measure when considering energy dissipation as it excludes the effect of spreading of the mass on R (Davies, 1982). Following studies such as Goujon et al. (2007), Yang et al. (2015), and Hu et al. (2020), the proportion of material was assigned by weight (rather than volume). Therefore, also due to the differences in mass configuration (i.e., pore spaces between the coarse particles are sometimes void and sometimes filled by the finer particles), the volume of the material was not identical in all experiments, as illustrated in Figure 2. Normalized runout (R_n) is used to illustrate and compare findings while accounting for the difference in volume by normalizing with the cubic root of the volume. The R_n is represented by the equations $R_n = R_f/h^*$ and the normalized propagation of the center of mass by $R_{nCoM} = R_{CoM}/h^*$, where the R_f and the R_{CoM} are normalized by the cubic root of the volume of the material ($h^* = V^{1/3}$). Davies and McSaveney (1999) suggest that such normalized quantities can be compared to real events. Total spreading (S_n) is measured as the normalized L of the deposit, $S_n = L/h^*$ (Manzella & Labiouse, 2013). The normalized distance between R_f and the propagation of the center of mass on the horizontal plane (R_{hCoM}) is also used here ($S_f = (R_f - R_{hCoM})/h^*$) as a measure of the spreading at the front of the avalanche (S_f), which is not affected by material left behind or piled on the slope during emplacement.

3.2. Scaling

Laboratory analog experiments have the potential to target and simulate mass flow processes. Nonetheless, they are brief, idealized, lack the complexity of geophysical systems (e.g., Baker, 1996) and cannot simulate the magnitude of their energy (Bowman et al., 2012; De Blasio & Crosta, 2014). Due to these limitations, careful planning, scaling and interpretation are necessary for rock/debris avalanche processes to be reproduced by analog experiments (Davies & McSaveney, 1999; Iverson & Denlinger, 2001; Iverson et al., 2004).

Scaling is critical in designing experiments and correlating the findings of small-scale granular avalanches to natural geophysical mass flows (Iverson, 2015; Iverson et al., 2004). Similarity between analog models and real events is addressed by introducing geometric and dynamic dimensionless parameters to satisfy the dimensional scaling of the components of the modeled system, the forces, and the continuum hypothesis (Iverson, 1997, 2015; Manzella & Labiouse, 2013; Shea & van Wyk de Vries, 2008). Geometric parameters refer to the dimensions and morphologies of the particles and the system. For the continuum hypothesis to be satisfied, enough particles should be present in the system to make the examined variables statistically valid, while particles are small enough to represent changes across them (Drake, 1991; Savage & Lun, 1988). Dynamic parameters refer to the ratio between forces within the avalanche, which are later addressed. The presented experiments follow the scaling considerations of the mentioned previous studies as outlined below. This was done to constrain the processes that have led to the proposition of bidispersity as a runout-enhancing factor. However, in the analysis of the experiments, the granular flow conditions were evaluated in terms of the effectiveness of their scaling.

First, particle size is large enough to reduce the impact of electrostatic effects to negligible levels (Drake, 1991; Iverson & Denlinger, 2001; Manzella & Labiouse, 2009). Additionally, it is assumed that there is a similarity to large-scale avalanches in terms of geometric shape, air and particle densities, and drag coefficient between particles and air (Davies & McSaveney, 1999). Moreover, Drake (1991) suggests that the avalanche depth needs

Table 1
The Five Experimental Series Examining Different Parameters

Experiment series	Gravel 9.5–16.0 mm	Gravel 16.0–22.4 mm	Sand 0.355–0.500 mm	Sand 0.500–1.000 mm	Mass (kg)	Inclination (°)
A	x	–	–	x	20	40
B	x	–	–	x	30	40
C	x	–	–	x	20	35
D	x	–	–	x	20	45
E	–	x	x	–	20	40

to be at least 10 times larger than the mean particle diameter, which is also fulfilled. These are the scaling guidelines most consistently followed by granular avalanche experiments and the present study. Geometric and dynamic scaling effects are further addressed in the discussion.

3.3. Material and Experimental Conditions

The material used in this study consists of four different particle sizes composed of subrounded gravels and subangular corundum sand (Text S1 in Supporting Information S2). Angular-subangular natural rock material is used in an attempt to maintain a close approximation to the modeled phenomena (Cagnoli & Romano, 2010; Davies & McSaveney, 1999; Li et al., 2021; Shea & van Wyk de Vries, 2008). Well-graded materials were sieved to produce size species with different particle sizes falling within a single sieve range. The coarse material in each experiment was composed of gravel of either 9.500–16.000 mm or 16.000–22.400 mm. In turn, the fine component is composed of sand of either 0.355–0.500 mm or 0.500–1.000 mm (Table 1). Different size species were then combined to create binary granular mixtures. The properties of the material used are reported in Text S1 of the Supporting Information S2. The material in rock/debris avalanches usually spans a wider size range and includes material of more sizes, rather than only the two species included in the binary mixtures included in these experiments. Additionally, the shape difference and frictional properties between the sand and the gravel are not representative of rock/debris avalanche material. However, particle shape is not the subject of the current study, and the material used allows reproducing the processes that caused enhanced mobility attributed to bimodality in previous studies. Size species with different roundness and frictional properties have been used by previous studies examining bidispersity, such as Phillips et al. (2006), to enhance and examine the same processes. The shape and friction angles of the material have a negligible effect on the processes considered in this study.

For the bidisperse experiments, a proportion (by mass) of finer granular material was added to the mass composed of coarser particles. For each set of experiments, this proportion ψ of fine material was varied between $\psi = 0$ (all coarse) and $\psi = 1$ (all fine). Prior to release, coarse and fine particles were placed in the release box so that the fine particles completely filled the pore spaces between the coarse particles from the bottom up (Figure 2). After placing a single particle thickness layer of the coarse material at a time, the pore spaces were filled with fines before repeating the process on the successive layer. In cases where low quantities of fine material were used, void pore spaces remained at the top of the material (Figure 2). Conversely, when the volume of the fines was greater than the pore space, excess fines were positioned above the coarse material.

For each ratio of fine material, other experimental parameters were changed to additionally investigate the potential effect of bidispersity under different conditions, and allow a better understanding of the effects of bidispersity. These parameters were volume, inclination and particle size. The experiments are divided into five series according to the parameters under examination as illustrated in Table 1. Each experiment was repeated a minimum of three times to generate data to be averaged and ensure repeatability.

4. Results

4.1. Morphology

Under all the conditions of bidisperse granular avalanches, the following common morphological features are observed. At low ψ values ($\psi < 0.5$ – 0.15 depending on experimental conditions) the addition of fines causes the final deposits to become longer initially (normalized length = L/h^*) and lower in height (normalized average height = average height/ h^*) compared to avalanches composed solely of coarse particles (e.g., Figure 3). They

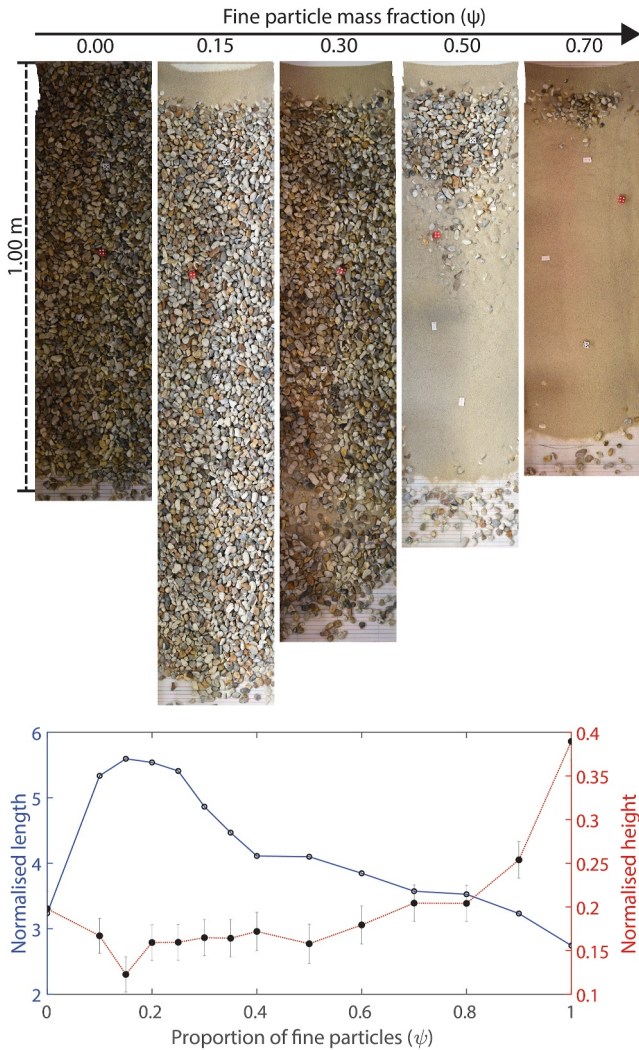


Figure 3. TOP: Orthophotos of the deposits of experimental avalanches in series A illustrating their runout and morphology. The flow direction is downward (The dice visible in the orthophotos are used as spatial reference, and as objects of known dimensions for the calibration of 3D models). BOTTOM: Normalized length (=length/volume^{1/3}) and height (=average height/volume^{1/3}) of the experimental avalanches of series A.

also achieved greater runouts (Figure 3: 0.00–0.15). At a critical value of ψ_{CRF} , maximum R_f is achieved (Figure 3: 0.15). However, further increase of ψ progressively results in a decreased R_f (Figure 3 > 0.15). With progressively higher ψ ($\psi > \sim 0.8$) a stage is reached where L is smaller and deposit thickness is higher than the monodisperse flow composed entirely of coarse particles. At low ψ values, coarse particles travel with the fine particles forming a continuous cover over the deposit surface (Figure 3: 0.00–0.30). At higher ψ they are emplaced at the rear of the deposit near the slope-break (Figure 3: 0.50–0.70). An exception arises when coarse particles that separate from the avalanche early and travel independently are deposited in front of it.

4.2. Frontal Velocities

For the purposes of the analysis of propagation dynamics and energy dissipation, avalanche propagation has been divided into three phases these phases considered separately. The V_f is divided into three parts. These phases are exhibited, with variation according to the experimental conditions, in all the experiments (Figure 4):

PHASE 1—ACCELERATION ON THE INCLINED SLOPE: This is the stage of acceleration following the release of the material. This phase ends when the front of the avalanche interacts with the slope-break to begin its transition to the horizontal plane.

PHASE 2—INTERACTION WITH THE SLOPE-BREAK: This phase begins when the front first interacts with the geometric irregularity of the slope-break and suffers a deceleration. This is followed by a rapid acceleration as the material behind the front (greater in mass) transfers momentum to the front. This can be observed in the video frames of the avalanches illustrated in Figure 5. Once the acceleration reaches peak velocity (V_{MAX}) in phase 2, and starts decelerating again, phase 2 ends. This is when the material at the front stops receiving energy directly from the momentum of the material interacting with the slope-break. The peak velocity V_{MAX} in phase 2 is not reached again by the flow.

Phase 2 deceleration is calculated here as the rate of velocity change between the interaction of the front with the slope-break (V_0) and the recording of the minimum velocity of phase 2 (V_{MIN}), as in the equation:

$$\text{Phase 2 percentage deceleration} = \frac{V_0 - V_{MIN}}{V_{MIN}} \quad (1)$$

where V_0 is the frontal velocity at the slope-break, and V_{MIN} is the lowest frontal velocity of phase 2 (Figure 4). Phase 2 acceleration is calculated as the rate of velocity change between the lowest velocity of phase 2 and the velocity of the front at the end of phase 2 (V_{MAX}):

$$\text{Phase 2 percentage acceleration} = \frac{V_{MAX} - V_{MIN}}{V_{MIN}} \quad (2)$$

where V_{MAX} is the velocity the front accelerates to at the end of phase 2 (Figure 4).

PHASE 3—DECELERATION AND EMLACEMENT: After the interaction with the slope-break stops disturbing the front of the flow, a deceleration phase eventually leads to emplacement. This phase is characterized by pulses of deceleration of the frontal material and subsequent acceleration (Figure 4). The V_f is lower for each subsequent pulse. Phase 3 ends when the material comes to a halt after losing momentum and energy and each particle settles

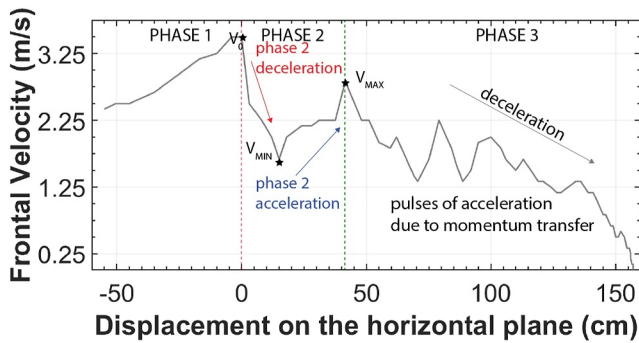


Figure 4. The frontal velocity of the avalanche with a fine particle content of $\psi = 0.15$ of experimental series B with the velocity phases annotated. V_0 : frontal velocity at the slope-break; V_{MIN} : lowest frontal velocity of phase 2; V_{MAX} : velocity the front accelerates to at the end of phase 2. Velocity uncertainty related to the measuring system: $\pm 0.25 \text{ ms}^{-1}$.

in its position in the final deposit. Phase 3 deceleration is calculated here as the average rate of velocity change between the initiation of phase 3 and the final deposition (Figure 4):

$$\text{Phase 3 average deceleration} = \frac{V_{MAX}}{\text{time duration of phase 3}} \quad (3)$$

4.3. Fine Particle Content (ψ)

Experiment series A (Table 1) has the primary aim of examining the impact of ψ on the runout and the mobility of the center of mass. It is also the reference case for the rest of the experiments. Figure 6a illustrates that changes in ψ result in variation of both the R_n and R_{nCoM} propagation metrics. The initial addition of fines for $\psi = 0.10$ leads to an increase in R_n and R_{nCoM} . The maximum R_n exhibited at $\psi_{CRf} = 0.15$ represents an increase of 87% from the all-coarse avalanche. In the case of the center of mass, at $\psi_{CRcom} = 0.10$ the equivalent increase is $\sim 100\%$. Therefore, there is a difference in ψ value for the maximum R_n in comparison to the maximum R_{nCoM} . Further increases in

ψ , past ψ_{CRf} and ψ_{CRcom} , result in reduced R_n and R_{nCoM} (Figure 6a). The greatest R_n and R_{nCoM} variability is observed at ψ between 0.10 and 0.35. However, R_n and R_{nCoM} remain above the all-coarse avalanche up to $\psi = 0.80$. The sensitivity of R_n and R_{nCoM} to ψ decreases after all the pore spaces between the coarse particles are filled by fines at $\psi = 0.35$ (Figure 6a). These observations are confirmed by Figure 6b. The H/R and H_{CoM}/R_{CoM} measure propagation including the location of the mass before their release and confirm that the relationships are not an effect of the initial position of the center of mass. Figure 6c illustrates that spreading S_n and S_f are greatest at $\psi = 0.15$. Once the pore spaces are filled with fine particles ($\psi > 0.35$), ψ variation has less impact on spreading (Figure 6c). Particularly, the S_f remains almost constant after pore spaces are filled.

Vf observations suggest that ψ affects phase 2 (interaction with the slope-break) and phase 3 (deceleration and emplacement). There is no systematic impact on phase 1 (acceleration on inclined slope, Figure 6d). In phase 2, the deceleration after the slope-break is consistently increased with increasing ψ (Figure 6e). Phase 2 acceleration increases with ψ between 0.10 and 0.35. In this range, increases in ψ result in lower acceleration (Figure 6e). The average deceleration of the material in phase 3 (Figure 6f) is not systematically reduced at low ψ between 0.10 and 0.35 (pore spaces not fully filled). At higher ψ , the average deceleration increases throughout the range of ψ values.

4.4. Volume

Experiment series B (Table 1) examines the combined effect of bidispersity and volume. Bidispersity has the impact observed in series A also at the higher volume, increasing mobility (runout and center of mass

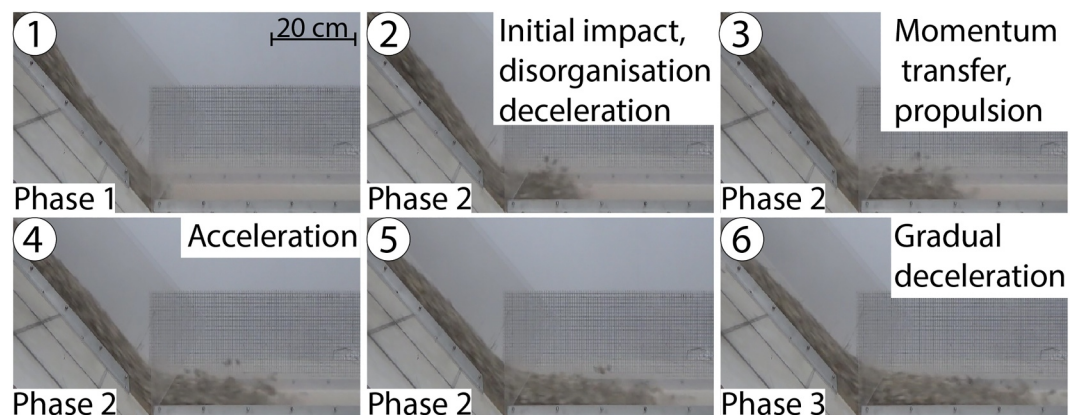


Figure 5. Frames from the interaction of the front of the avalanche ($\psi = 0.15$, series B) with the slope-break. The frames illustrate the phases of granular avalanche propagation.

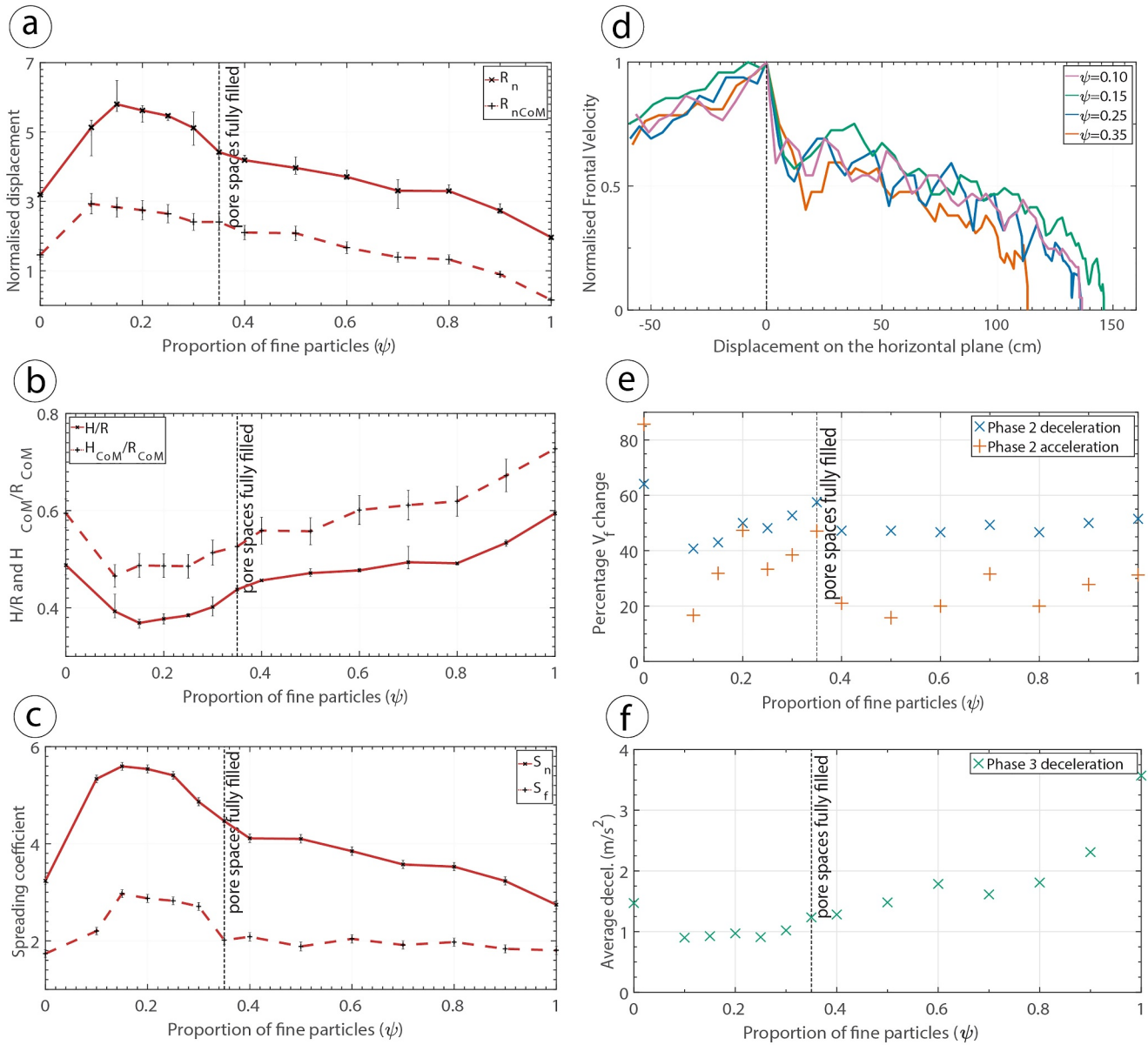


Figure 6. (a–c) Results from experimental series A. (a) Frontal runout (R_n) and propagation of the center of mass (R_{nCoM}) at different proportions of fines (ψ). (b) H/R and H_{CoM}/R_{CoM} at different ψ . (c) Total spreading (S_n) and frontal spreading (S_f) at different ψ . (d–f) Velocity results from experimental series A. (d) Velocity normalized by the maximum velocity achieved for 4 avalanches (Velocity uncertainty related to the measuring system: $\pm 0.25 \text{ ms}^{-1}$). Dashed horizontal line represents the location of the slope-break. The velocities of the rest of the experiments of series A are illustrated in Figure S3 of the Supporting Information S2. (e) Velocity change during the acceleration and deceleration of phase 2. (f) Phase 3 average deceleration.

displacement) at low ψ and progressively diminishing (Figure 7a). However, Figure 7a illustrates that with higher volume, R_n values are greater. Nonetheless, R_{nCoM} is not increased. This trend is confirmed by Figure 7b, illustrating H/R and H_{CoM}/R_{CoM} . Figure 7c suggests that spreading is greater for the higher volume avalanches.

Volume does not systematically affect V_f in phase 1 in comparison to series A. In phase 2, slope-break series B avalanches (lower volume) experienced similar deceleration on impact with the slope-break series A. However, the acceleration of phase 2 achieves higher velocities and lasts longer in higher volume avalanches (Figure 8).

In phase 3, pulses of acceleration and deceleration show a higher V_f amplitude in the higher volume avalanches. The V_{MAX} achieved in these pulses is greater at greater volumes. They are then decelerated and accelerated again to high velocities throughout phase 3 compared to the less voluminous series A (Figure 8).

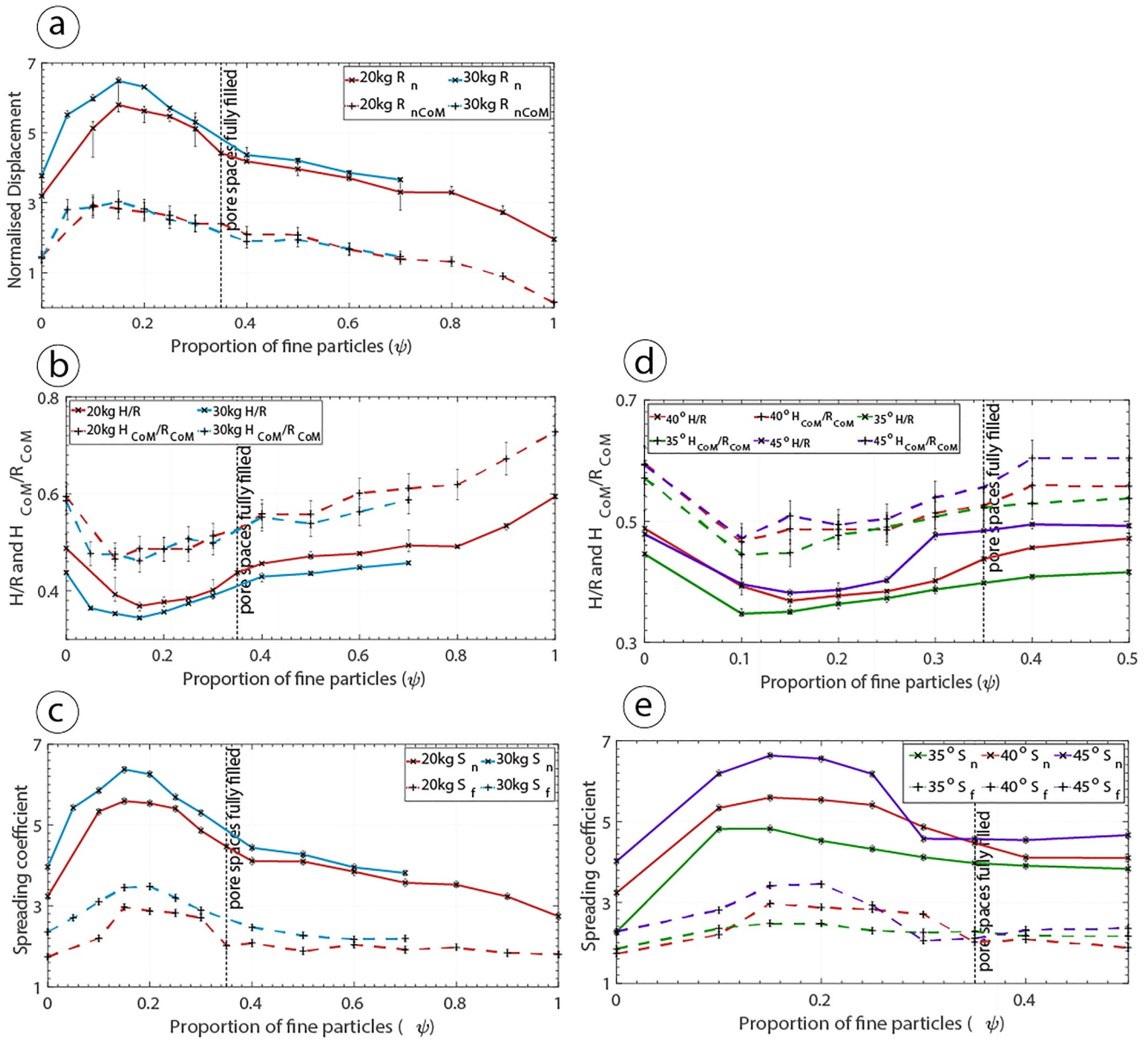


Figure 7. (a–c) Results from experimental series B. (a) Frontal runout (R_n) and propagation of the center of mass (R_{nCoM}) at different proportions of fines (ψ). (b) H/R and H_{CoM}/R_{CoM} at different ψ . (c) Total spreading (S_n) and frontal spreading (S_f) at different ψ . (d and e) Results from experimental series C and D. (d) H/R and H_{CoM}/R_{CoM} at different ψ . (e) Total spreading (S_n) and frontal spreading (S_f) at different ψ .

4.5. Inclination

For experiment series C and D (Table 1), the slope inclination was 35° and 45°, respectively, also altering the angle of the slope-break. By changing the inclined slope angle, the H —horizontal runout distance on the slope and the height of the center of mass prior to release are altered. For this reason, we use their H/R and H_{CoM}/R_{CoM} for comparison for series C and D (instead of R_n and R_{CoM}) instead of the runout. Figure 7d presents findings that suggest that between 35° and 45°, increased slope inclination generates less mobile avalanches, both in terms of their center of mass as well as frontal runout. Although the maximum mobility of the center of mass is achieved for all inclinations at $\psi_{CRcom} = 0.10$, in the case of the maximum R a deviation is observed. The maximum is at $\psi_{CRf} = 0.15$ for 40° and 45°, whereas it is at $\psi_{CRf} = 0.10$ for 35°. Spreading also differs, as illustrated in Figure 7e. The effect of bidispersity on the degree of spreading is more intense at low ψ , before all pore spaces are filled. Spreading is lowest for the 35° experiments, and increases progressively at higher inclinations.

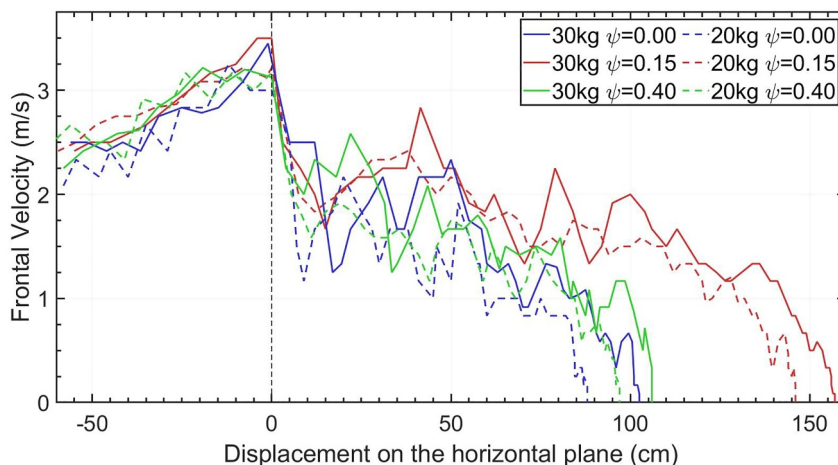


Figure 8. Frontal velocity comparison between the avalanches of series A (20 kg) and B (30 kg). Uncertainty related to the measuring system: $\pm 0.25 \text{ ms}^{-1}$.

4.6. Size-Ratio Between Particle Species (Δ)

In experimental series E (Table 1), the granular mixtures were composed of finer fine particles and coarser coarse particles, thus increasing the size ratio (Δ) between the species ($\Delta = \text{coarse particles mean diameter}/\text{fine particles mean diameter}$). Previous experimental series had a size ratio $\Delta = \sim 17$, whereas series E had a size ratio $\Delta = \sim 45$. Figure 9a illustrates that increased Δ results in greater R_n and R_{nCoM} at low ψ . Figure 9b, which also considers the difference in the center of mass prior to release due to the difference in their sizes, confirms that at low $\psi = 0.05$

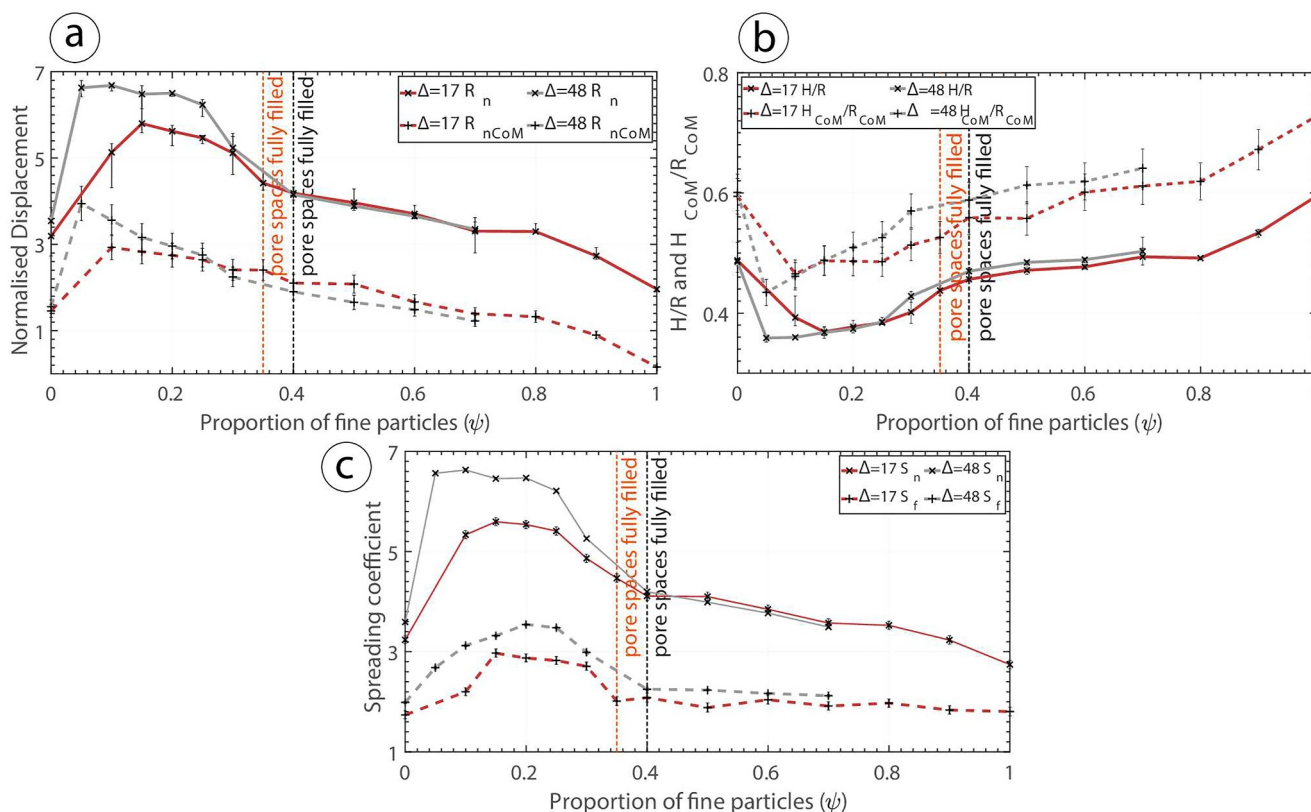


Figure 9. Results from experimental series E. (a) Frontal runout (R_n) and propagation of the center of mass (R_{nCoM}) at different proportions of fines (ψ). (b) H/R and H_{CoM}/R_{CoM} at different ψ . (c) Total spreading (S_n) and frontal spreading (S_f) at different ψ .

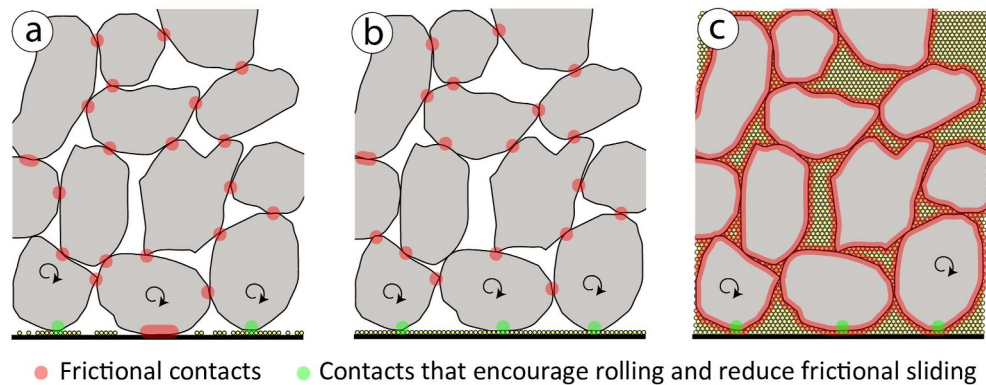


Figure 10. Types of contacts between the fine (yellow) and the coarse (gray) particles at different mixture proportions between them.

and $\psi = 0.10$ the granular mixture with greater Δ is more mobile in terms of R_n and R_{nCoM} . At ψ values greater than $\psi > 0.10$, series E avalanches with greater Δ are less mobile. The peak in R_n and R_{nCoM} for experiment series E comes at $\psi_{CRf} = \psi_{CRcom} = 0.05$, compared to $\psi_{CRcom} = 0.10$ and $\psi_{CRf} = 0.15$ for series A. In series E, spreading is greater for all ψ values when only the front of the deposit is considered (S_f) (Figure 9c). When the entire length of the deposit is considered (S_n), the spreading of flows from series A and E is very similar after the pore spaces between the coarse particles are filled by fines.

A more detailed discussion of the observation of the granular avalanches with different volumes, slope inclinations and Δ is expanded in Text S2 of the Supporting Information S2. The document includes an analysis of the granular processes under the stated conditions and a comparison with experimental series A.

5. Discussion

5.1. Bidispersity and Mobility in Small-Scale Granular Avalanches

The findings are in agreement with previous studies reporting increased runout in granular avalanches composed of bidisperse mixtures compared with monodisperse (e.g., Bartali et al., 2020; Degaetano et al., 2013; Moro et al., 2010; Phillips et al., 2006; Roche et al., 2006; Yang et al., 2015). Maximum runouts are recorded at different proportions of ψ in different experiments as a function of parameters such as Δ and slope inclination. In agreement with previous studies (e.g., Phillips et al., 2006), it is observed that at low ψ fine particles position themselves at the bottom of the avalanche through kinetic sieving. Observations confirm the propositions of Goujon et al. (2007) that segregation is a very fast process in bidisperse mixtures at the scale of these experiments. At high values of ψ , observations and footage support that coarse particles are unable to travel independently as they are trapped in the mass of fine particles, generating a sand-trap absorbing their kinetic energy (Figure 3) (Bartali et al., 2020; Phillips et al., 2006). Thus, coarse particles are deposited on top of the fine particles close to the slope-break (Figure 3a).

The observed increased runout at low ψ values, and subsequent increase at increased ψ , combined with the observed segregation and behavior of the size species are in agreement with the reduction of basal friction hypothesis proposed by previous studies. Based on the interpretation of analog and numerical experiments, these studies suggest that fine particles located at the base reduce frictional contact areas between the coarse particles and the substrate, acting as ball-bearers (e.g., Linares-Guerrero et al., 2007; Oda & Kazama, 1998; Roche et al., 2006), and encourage rolling as opposed to frictional sliding (Phillips et al., 2006). This process reduces the effective friction coefficient at the base of the flow and inhibits frictional energy losses (Hu et al., 2020, 2021; Phillips et al., 2006). These processes would result in the increased R_n and R_{nCoM} observed in this study. In series A, this process is most efficient at $\psi = 0.10$ where maximum R_{nCoM} occurs (Figure 6a). At lower ψ values (<0.10 in series A), there are not enough fine particles to optimally lubricate all frictional contact surfaces at the base of the flow as not all coarse particles are supported by fines (Figure 10a) (Moro et al., 2010). The numerical modeling of Linares-Guerrero et al. (2007) suggests that the most efficient arrangement is one with a single particle size thickness layer continuous sheet of fines at the base of an avalanche. In such a case, the basal contacts

are lubricated, but no particles are present within the avalanche body, as illustrated in Figure 10b (Moro et al., 2010). This is confirmed by the observation of a layer of fine particles in the more mobile experiments of the current study (Figure 3: $\psi = 0.15$).

As ψ increases (>0.10), fines cover the base and start filling pore spaces between the coarse particles within the avalanche. Interparticle frictional contact surfaces increase as the pore spaces between the coarse particles are filled (Figures 2 and 10c). This progressively inhibits R_n and R_{nCoM} further with subsequent ψ increases as illustrated by Figure 6a, supporting the trend reported in other studies (Bartali et al., 2020; Hu et al., 2020, 2021; Moro et al., 2010; Phillips et al., 2006; Yang et al., 2011). The findings support that increased frictional losses in the interparticle contacts begin to offset the energy conserved at the base (Hu et al., 2020; Moro et al., 2010). However, it is important to note that even after all the pore spaces between coarse particles are filled ($0.35 > \psi < 0.80$ for series A), bidispersity enables mobilities greater than the monodisperse avalanches with all-coarse or all-fine particles (Figure 6a). The ψ_{CRf} has been suggested by various experimental studies to be between 0.05 and 0.50 (e.g., Degaetano et al., 2013; Hu et al., 2020; Moro et al., 2010; Roche et al., 2006; Yang et al., 2015). In the current experiments, it is $\psi_{CRf} = 0.15$ in the majority of cases; however, it changes to $\psi_{CRf} = 0.10$ for the 35° slope inclination (exp. series C) and $\psi_{CRf} = 0.05$ for the experiments with greater Δ (exp. series E). Therefore, ψ_{CRf} is a function of the geometry of the flow path and Δ , according to the parameters examined here.

The ψ affects the propagation of the center of mass by basal lubrication. However, the spreading of the mass is affected in a process that appears to be independent as they do not follow the same trend (Figures 6, 7, and 9) and ψ_{CRf} does not always coincide with ψ_{CRcom} . Greater runout does not necessarily imply greater propagation of the center of mass. Investigating R_{CoM} reflects energy dissipation and is therefore more appropriate for investigating the energetics of granular flows (Legros, 2002). In fact, H/R is mechanically irrelevant as a measure of mobility, since spreading can produce higher runouts irrespective of the center of mass, and therefore kinetic energy dissipation (Davies, 1982; Dufresne et al., 2021; Legros, 2002). Furthermore, in agreement with the monodisperse granular experiments of Manzella and Labiouse (2009), in series B with increased volume, the increased R_f does not match the R_{CoM} . Examination of the avalanche spreading at different volumes in Figure 7c suggests that the greater R_n at higher volumes results from greater spreading generating longer deposits even though the R_{CoM} is similar, as also reported by Li et al. (2021) and Yang et al. (2011). Thus, as initially suggested by Hsü (1975), the interpretation of the H/R (or *Fahrböschung*) as the friction angle is inappropriate when considering energetics, and should instead be measured as the inclination of the line connecting the center of gravity of the material pre-release and post-deposition (H_{CoM}/R_{CoM} or energy line gradient) (Figure 1b).

Vf observations suggest that ψ affects the interaction of the avalanche with the slope-break (phase 2) and the subsequent propagation on the horizontal plane (phase 3), as also supported by the experimental study of Fan et al. (2016). Small ψ values drastically lower phase 2 deceleration and the average deceleration rate of phase 3 compared to monodisperse endmembers (Figures 6e and 6f). Velocity measurements and video observations support the idea that the interaction of the avalanche with the slope-break causes loss of momentum (also observed by Crosta et al. (2017)) and disorganization in the particle position in the mass (Figure 5) (also observed by Manzella and Labiouse (2009)). The impact of path irregularities on granular avalanche propagation has been previously highlighted by researchers such as Heim (1932), Pudasaini et al. (2005), and Manzella et al. (2013). The slope-break causes an increase in shear and loss of momentum (Crosta et al., 2017) with energy lost outside the avalanche system. Increased slope angles generate a greater path irregularity, collisions and energy dissipation as illustrated by the results of experimental series C and D (and further expanded in Text S2 of the Supporting Information S2). Fan et al. (2016) observed more pronounced decelerations in phase 2 at lower particle sizes. In accordance, the deceleration of the fine particles in phase 2 of the current experiments leads to accumulation of material at the toe of the slope. This is the result of the greater size ratio between particles and the slope-break discontinuity (Manzella & Labiouse, 2013). Furthermore, momentum transfer from the rear was not efficient at high ψ values as the accumulated fines acted as a sand-trap (Bartali et al., 2020; Fan et al., 2016). However, at greater ψ values ($\psi > 0.25$) the R_{nCoM} is lower in the experiments with higher Δ . This is the result of the smaller fine particles losing more energy at the slope-break, suffering greater deceleration in phase 2 due to the greater size ratio between the particles and the slope-break (Fan et al., 2016). Fine particles in sufficient quantities ($\psi > 0.25$) can absorb the momentum of coarser particles, making the kinetic energy transfer in phase 2 less efficient. Nonetheless, the lower deceleration rate observed in experimental series A phase 3 at $\psi < 0.7$ (Figure 6f), after the slope-break plays a role, supports that the addition of fine particles imposes a more efficient

flow arrangement. Pulses of acceleration and deceleration of the front observed in phase 3 (e.g., Figures 4, 6d, and 8) have also been described by Van Gassen and Cruden (1989) and Bartali et al. (2015). Van Gassen and Cruden (1989) suggest that as the leading material decelerates due to friction, the approaching material from further back has not yet experienced equal retardation. The leading material deceleration leads to an interaction of momentum transfer through impact (Hu et al., 2021; Van Gassen & Cruden, 1989). The leading particles are propelled forward while the following material is decelerated to lower velocities. It can be observed by careful examination of the experiment videos in the current study and has also been reported in the experiments of Manzella and Labiouse (2009—monodisperse) and Yang et al. (2011—bidisperse/polydisperse). The cyclic recurrence of this process is evident through V_f oscillation pulses (Figure 8). The collisions are strongly inelastic, consuming kinetic energy (Hergarten, 2024), and therefore each subsequent pulse achieves lower velocities as the energy in the system is depleted. By using energy equations to describe the momentum transfer occurring in these processes, Van Gassen and Cruden (1989) produced a model that suggests that a granular mass interacting in this manner results in significantly longer runouts (>1.5 times longer) than predicted by simple sliding block models with no momentum transfer. However, a collisional regime is required for this process. The transfer of momentum from the rear to the front causes the mass to spread and the front of the flow to travel farther. The findings suggest that the reduced frictional energy dissipation that fine particles enable at the base makes more energy available as kinetic and reduces the deceleration of the material in phase 3, generating longer runouts.

5.2. Scaling, Granular Flow Regimes and Kinetic Sieving—Implications for Rock/Debris Avalanches

Rock/debris avalanches generate horizontal runouts greater than the initial fall height (Hung, 2002; Legros, 2002; McSaveney et al., 2000). This feature was recreated in the presented experiments with H/R values as low as 0.35. Although long-runout avalanches are difficult to recreate at the lab scale (Friedmann et al., 2006; Manzella & Labiouse, 2013), in the granular avalanches presented in this study R_n values >6.5 have been achieved with bidisperse mixtures, compared to $R_n = 3.2$ – 3.3 that is the maximum achieved by most monodisperse end-member avalanches. These values are in line with values exhibited by some natural rock/debris avalanches such as the Elm (Switzerland) ($R_n = 5.1$) and Frank (Canada) ($R_n = 5.6$) rock avalanches (Hsü, 1978; Manzella & Labiouse, 2013). However, the appropriateness of such comparisons is discussed in the final section of the discussion.

5.2.1. Scaling of Experiments

Small-scale experiments are not capable of reproducing some of the processes enabled at the scale of natural geophysical flows (Iverson et al., 2004). Naturally, laboratory experiments cannot simulate fragmentation processes due to the low energies in the system (Bowman et al., 2012; De Blasio & Crosta, 2014) or the seismicity of the events (Davies & McSaveney, 1999). Even so, if fluid effects are negligible, major features of rock/debris avalanches can still be reproduced by analog experiments with appropriate scaling since their dynamics are principally controlled by the internal and basal friction coefficients and the interaction of the avalanche with its path (Davies & McSaveney, 1999; Dufresne, 2012; Iverson & Denlinger, 2001; Iverson et al., 2004; Yang et al., 2011). However, skepticism regarding the effectiveness of small-scale experiments centers around their being too brief, idealized and restricted by initial conditions and artificial boundaries to represent the vast complexities of natural geophysical processes (e.g., Baker, 1996). Iverson (2015) caution that the geomorphological relevance of small-scale granular flow experiments carried out in the past decades (e.g., Iverson et al., 2004; Mangeney et al., 2010; Pudasaini & Hutter, 2007) should be critically evaluated, in terms of scaling and interpretation in comparison to natural processes, before being extended to direct comparison with natural phenomena. The same caution has to be dedicated to the scaling of bidisperse granular flows.

Assessment of experimental scaling is essential in designing and interpreting the findings of granular avalanche experiments regarding their geomorphological and mechanical relevance to the dynamics of rock/debris avalanches (Iverson, 2015). Other than geometric scaling parameters, dynamic scaling parameters refer to the ratio between forces within the body of a granular avalanche and describe the evolving dynamics of the system. However, this scaling aspect of experimental design is very frequently overlooked (Iverson, 2015). Nonetheless, since the perfect correspondence between physical experiments and real events is not possible, some distorted scale effects are introduced (Heller, 2011) and have to be mitigated. The potential scale-dependence of the simulated conditions must be assessed and is thus discussed in the subsequent sections. At the scale of these experiments, rolling motion at the base of the avalanche generates agitation and collisions between particles,

leading to a collisional regime, as also described by Hu et al. (2021). The flow regime was initially qualitatively assessed in the current experiments through real-time observation and the videos. The collisional and frictional regimes, introduced by Drake (1990, 1991), describe a difference in the behavior of propagating granular avalanches. In a frictional regime, the majority of the propagation particles are engaged in persistent frictional contacts, responsible for the majority of momentum transfer. In an avalanche under this regime, the majority of the material propagates as a coherent plug over a basal agitated zone. Plug behavior implies a coherent state, lacking agitation and significant shear stresses. In contrast, in the collisional regime, the majority of momentum transfer is due to frequent particle collisions in an agitated mass with a high granular temperature (Drake, 1991; Legros, 2002; Manzella & Labiouse, 2013). Different regimes and resultant granular behavior (i.e., particle interaction frequency, duration, etc.) alter the energy dissipated by avalanches and their mobility (Cagnoli & Piersanti, 2015).

The Savage number (N_{Sa}) is the ratio between particle collision stress and the load on the bed due to the weight of particles and can be approximated as:

$$N_{Sa} \approx \frac{u^2 \delta^2}{gT^3} \quad (4)$$

where u is the maximum speed (ms^{-1}), δ is the typical particle diameter (m), g is the gravitational acceleration (ms^{-2}) and T is the avalanche thickness (Iverson, 1997; Iverson et al., 2004). The typical particle diameter is characterized as the volume averaged mean diameter D_{43} (Breard et al., 2020; Gu et al., 2016), calculated as

$$D_{43} = n_q d_q \quad (5)$$

where n_q is the mass fraction of a particle class q with diameter d_q . The volume-averaged mean diameter has been found to be a suitable characterization for flows of binary mixtures (Rognon et al., 2007; Tripathi & Khakhar, 2011).

N_{Sa} is a non-dimensional characterization of the flow regime, differentiating between the frictional ($N_{Sa} < 0.1$) and collisional regime ($N_{Sa} > 0.1$) by quantifying the relative importance of inertial stresses over the total stresses in steady, gravity-driven flows with free upper surfaces (Hsu et al., 2014; Iverson, 2015; Iverson & Vallance, 2001; Iverson et al., 2004; Savage, 1984; Savage & Hutter, 1989). Greater N_{Sa} values imply significant collisional stresses, while when low, the regime is frictional and friction-dominated (Iverson & Vallance, 2001; Savage & Hutter, 1989).

Two important factors for the N_{Sa} are the typical particle diameter δ and avalanche thickness T (Equation 4). The flume tests of Cagnoli and Romano (2012) and Cagnoli and Piersanti (2015) suggest that changes in the mobility of small-scale granular avalanches triggered by particle size and volume changes are, in fact, due to the resultant variation of granular agitation and the N_{Sa} . The agitation and nature of particle interactions is a principal factor for energy dissipation and should be considered when interpreting avalanches (Li et al., 2021). Indeed, avalanches in this study with different ψ (Table 2) have variable δ and T , according to the proportion of each particle size species. For experimental series A, the N_{Sa} was calculated for their propagation on the horizontal plane after the slope-break. For the majority of the experiments, the N_{Sa} is above 0.1 (Figure 11a), confirming that the material propagated under a collisional regime which is not representative of rock/debris avalanches with N_{Sa} values typically much lower than 0.1 (data collected and presented in Appendix Table 2 of Li et al. (2021)). Only experiments with $\psi > 0.80$ result in N_{Sa} values in the frictional regime (Figure 11a).

The T component of the N_{Sa} equation is directly correlated with the number of particles in an avalanche (assuming equal δ). The system-to-particle size ratio proposed by Cabrera and Estrada (2021) is essentially a proxy for the number of particles in a granular system. Similarly, a system-to-particle volume ratio is here defined as the ratio of the volume occupied in the mass by a single particle of mean diameter when assuming spherical particles arranged in simple cubic packing to the total volume of material:

$$\text{system} - \text{to} - \text{particle volume ratio} = \frac{V}{4\sqrt{2}\left(\frac{\delta}{2}\right)^3} \quad (6)$$

Table 2
Experimental Series A—Savage Number, System-To-Particle Volume Ratio and Information Required for Their Calculation

ψ	δ (m)	Volume (m ³)	T (m)	System-to-particle volume ratio	Savage number
0.00	0.0128	0.0168	0.06	1.1E + 04	0.773
0.10	0.0116	0.0157	0.057	1.4E + 04	0.740
0.15	0.0110	0.0152	0.054	1.6E + 04	0.782
0.20	0.0104	0.0148	0.055	1.9E + 04	0.662
0.25	0.0098	0.0145	0.051	2.2E + 04	0.736
0.30	0.0092	0.01388	0.055	2.6E + 04	0.517
0.35	0.0086	0.0128	0.051	2.9E + 04	0.566
0.40	0.0080	0.0115	0.0483	3.2E + 04	0.576
0.50	0.0068	0.0109	0.045	5.0E + 04	0.514
0.60	0.0056	0.0123	0.051	1.0E + 05	0.239
0.70	0.0044	0.0137	0.051	2.4E + 05	0.147
0.80	0.0032	0.0141	0.063	6.4E + 05	0.041
0.90	0.0020	0.0132	0.0645	2.5E + 06	0.015
1.00	0.0008	0.0133	0.03	4.5E + 07	0.021

Note. ψ : mass proportion of fines; δ : characteristic particle size diameter; T: avalanche thickness.

The system-to-particle volume ratio of the presented experiments is similar to the experiments previously mentioned (Table S1 in Supporting Information S2). Li et al. (2021) proposed a negative correlation between the system-to-particle volume ratio and the N_{Sa} , which is also supported by series A of the experiments of this study (Figure 11b), supported by a high R^2 value of 0.89. Li et al. (2021) find that increasing the volume and decreasing δ have the same effect since they both affect the system-to-particle volume ratio. The findings of Cabrera and Estrada (2021) support that with sufficiently large system-to-particle-volume ratios (expected in natural avalanches), the mobility and shear strength of granular column collapses are independent of particle-size distribution variations. As granular systems become larger, particle size effects weaken (Cabrera & Estrada, 2021). Consequently, small system behavior can be biased by small system-to-particle volume ratios and flow height, resulting in high N_{Sa} values and energy exchange dominated by collisions. Such conditions are unrepresentative

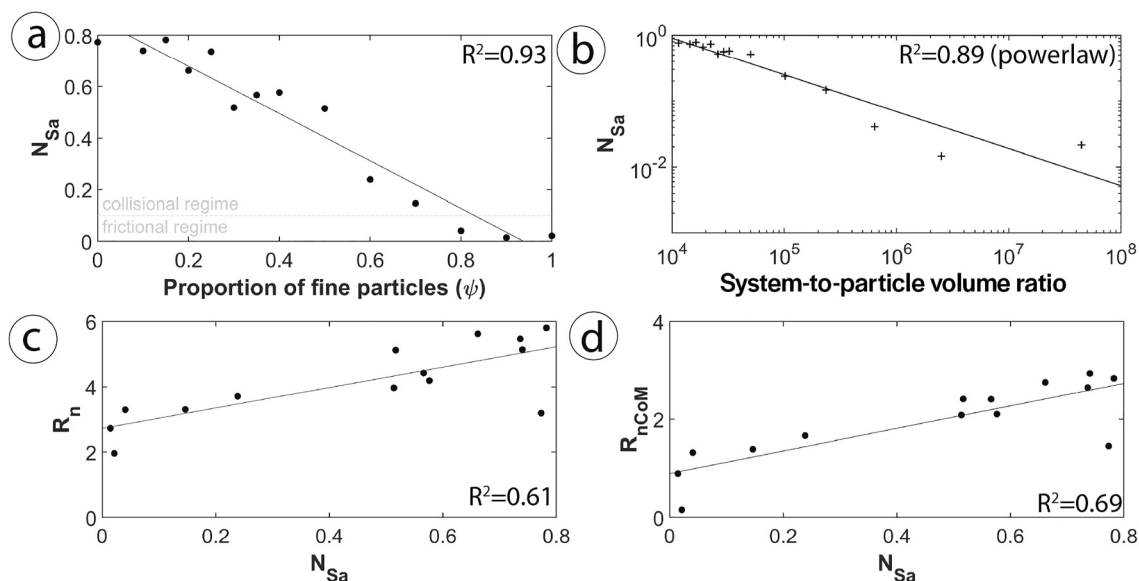


Figure 11. Scaling evaluation of experimental series A. (a) N_{Sa} as a function of ψ . (b) N_{Sa} as a function of the system-to-grain volume ratio. (c) R_n as a function of N_{Sa} . (d) R_{nCoM} as a function of N_{Sa} .

of natural processes (Cabrera & Estrada, 2021; Li et al., 2021). With small numbers of particles, agitation is greater per unit of flow mass since agitation is able to propagate up from the base and agitate a higher proportion of the avalanche (Cagnoli & Romano, 2010, 2012). Li et al. (2021) observed that a reduction of δ or increase in volume led to localization and magnification of shear stress at the base of the avalanche, leaving the overriding material to travel as a plug with no agitation. This is also observed in numerical simulations of granular avalanches (e.g., Silbert et al., 2001; Walton, 1993). The N_{Sa} of the plug is zero, resulting in extremely low overall N_{Sa} values in such avalanches (Li et al., 2021).

Small system-to-particle volume ratios can lead to behaviors unrepresentative of large-scale events due to the small number of particles involved in the experimental systems (particle size effect) rather than the particle-size composition and distribution (Cabrera & Estrada, 2019, 2021; Li et al., 2021). The increase in the R_n and R_{CoM} observed in avalanches from this study exhibits a correlation with the N_{Sa} (Figures 11c and 11d). The low coefficient of determination values of 0.61 and 0.69 respectively suggest that ~30%–40% of the variance in R_n and R_{CoM} cannot be attributed to the N_{Sa} . However, the covariance suggests that factors impacting the N_{Sa} and the collisional regime dynamics of the flow might be responsible for the variability in propagation, instead of ψ being the exclusive factor.

High N_{Sa} values and the observation of collisional behavior are very frequent in the reporting of lab-scale granular avalanche experiments. Li et al. (2021) calculate and report that N_{Sa} values of their experiments reflect a frictional regime for the majority of their experimental conditions. However, in the experiments of Cagnoli and Romano (2012), N_{Sa} is reported to have been larger than the threshold of 0.1. Lai et al. (2017), Bartali et al. (2020), and Duan et al. (2022) report their qualitative observation of collisional behavior without further examining or commenting on the implications of this behavior for comparison with natural events. However, the estimated N_{Sa} values of natural rock/debris avalanches are typically much lower than 0.1 (data collected and presented in Appendix Table 2 of Li et al. (2021)). A uniform collisional regime does not occur in large rock/debris avalanches and thus shear stresses are dissimilar to small-scale avalanches (Iverson et al., 2004). Therefore, the current experiments, as well as a large part of lab-scale granular avalanche experiments, generate a collisional regime, resulting in dynamics and shear stresses which are scale-dependent and should not be extended to comparison with rock/debris avalanches.

Therefore, caution and a rigorous approach are crucial in their design and the interpretation of analog experiment results (Iverson, 2015). Geomorphological and mechanical relevance should not be assumed on the basis of superficial or morphometric similarity, as it does not necessarily imply similarity in processes as exemplified in the analysis of this work (Iverson, 2015). Dynamic scaling analysis must become a standard procedure in designing and interpreting analog granular avalanche experiments to ensure the effectiveness of the experiments in examining the desired processes and dynamics. To achieve geomorphological and mechanical relevance, experiments on rock/debris avalanches require large enough scales (number of particles/avalanche thickness) to permit frictional regime behavior (Iverson & Denlinger, 2001). Analog experiments aimed at the study of rock/debris avalanches should ensure that the material involved generates a system-to-particle volume ratio which is small enough to permit an N_{Sa} smaller than 0.1, and therefore a frictional regime. This will depend on the properties of the material used such as the coefficient of restitution (e.g., Schilirò et al., 2019). If these properties are not well constrained, the flow regime may need to be evaluated after the experiments, as has been done for the current experiments, to ensure a frictional regime. A pilot study, examining the dynamics of granular systems could benefit experiments where the conditions are not well constrained. However, it is vital that the force balance is consistent with the processes targeted as well as the geometrical scaling.

5.2.2. Granular Avalanche Propagation Processes: Comparison at Different Scales and Implications for Rock/Debris Avalanches

The bidispersity-enhanced mobility hypothesis requires fine particles at the flow base, making segregation essential for enhanced mobility. However, segregation is not generally observed in large rock/debris avalanche deposits which achieve the longest runouts, and it is no longer believed that they are dominated by chaotic particle collisions and high granular temperatures (e.g., Dufresne et al., 2016; Dunning, 2006; Makris, Roverato, Dávila-harris, et al., 2023; Makris, Roverato, Lomoschitz, et al., 2023; Makris et al., 2020; Paguican et al., 2021). Although some studies do report grading at the deposit scale (e.g., Crosta et al., 2007; Hewitt, 1998), others observe the lack of it (e.g., Makris, Roverato, Dávila-harris, et al., 2023; McSaveney, 1978; Schilirò et al., 2019;

Shreve, 1966). Grading has been more commonly observed in deposits which are orders of magnitude smaller than the largest rock/debris avalanches (e.g., Marc et al., 2021: $<10^{-5}$ – 10^{-3} km³). However, other work supports that in larger events grading is a bias introduced by the presence of a coarse carapace at the top of rock avalanche deposits and does not persist lower in their body (Dufresne & Dunning, 2017; Dunning, 2006; Dunning & Armitage, 2011). In any case, not all long runout rock/debris avalanches exhibit widespread segregation and grading and therefore a process that requires them cannot be the only factor for long runouts. In the current experiments, the process that generates the segregation is kinetic sieving. The granular mass dilates during the agitated motion with voids opening between the coarse particles for the finer particles to percolate through to the base due to gravity (Savage & Lun, 1988). Hu et al. (2021) propose that, similar to lab experiments, kinetic sieving allows fine particles to migrate to the base and lubricate rock/debris avalanches. This is based on the idea prevalent in the past that rock/debris avalanches were envisaged as rapid granular flows with their dynamics dominated by chaotic and energetic particle collisions (De Blasio, 2011) and a collisional regime. Accordingly, some researchers have suggested that rock/debris avalanches are efficient at sorting particles by size (e.g., Savage & Lun, 1988). This would lead to inverse grading observed across all deposits (Cruden & Hungr, 1986; Dufresne, 2009; Hungr & Evans, 2004; Middleton, 1976), which is not commonly observed in large events. The lack of grading in the majority of long runout rock/debris avalanches suggests that flow dynamics differ with the analog avalanches. The hypothesis of a bidisperse basal low friction zone supporting of a plug above it is also disputed by the observation of shear zones throughout the body of some rock/debris avalanche deposits at various depths (e.g., Dufresne & Dunning, 2017; Dufresne et al., 2016; Hughes et al., 2020; Makris, Roverato, Dávila-harris, et al., 2023; Roverato et al., 2015; Wang et al., 2019) confirming that shear is not always exclusively accommodated at their base. Therefore, the sedimentological evidence disputes the action of segregation placing finer particles at the base and enabling them to enhance mobility.

Additionally, recent analog experiments by Polanía et al. (2023) support the previous numerical (e.g., Cabrera & Estrada, 2021; Estrada, 2016; Zhu et al., 2020) and experimental (e.g., Li et al., 2015; Yang & Luo, 2018) studies suggesting that in sufficiently large system-to-particle volume ratios the shear strength and residual friction angles of non-segregated granular mixtures is independent of their particle-size distribution and size ratio Δ . Therefore, in unsegregated large system-to-particle volume ratio systems bidispersity is unlikely to affect the apparent friction coefficient. Schilirò et al. (2019) propose the existence of dimensional limits for kinetic sieving owing to flow regime being scale dependent according to velocity and particle number/flow thickness. Agitation throughout the material is essential for kinetic sieving to enable the inverse grading and runout enhancing process with the fine particles at the base. At lab-scale low system-to-particle volume ratios, a collisional regime is attained; however, flows with an agitated basal layer and the areas above traveling as a plug (frictional regime) develop at large system-to-particle volume ratios equivalent to large rock/debris avalanches. The lack of kinetic sieving in a frictional regime prevents segregation. Based on the above line of evidence, size segregation may not occur in most rock/debris avalanches to enable the processes observed in analog experiments; therefore, other processes should be investigated to explain rock/debris avalanche long runouts.

6. Conclusions

Analog granular flow experiments were carried out in a scaled setup to investigate the effects of bidispersity on granular avalanche propagation processes and dynamics. Analysis of the findings leads to the following conclusions:

- Bidispersity has the potential to affect energy dissipation in granular avalanches and increase their runout at the scale of the considered experimental conditions. It was found that low ψ values between $\psi = 0.05$ and $\psi = 0.15$ (depending on experimental conditions) are most efficient at enhancing mobility. At higher ψ values, up to $\psi = 0.80$, the mobility is still greater than $\psi = 0.00$.
- Runout is affected by both the displacement of the center of mass as well as the spreading of the mass.
- The effect of bidispersity is altered according to the slope inclination before the horizontal depositional surface. However, it is not affected by the volume of the material. Spreading is also affected by the inclination of the slope before the horizontal depositional surface and the angle of the slope-break. Increases in runout with increased volumes are the result of enhanced spreading.
- The increase in mobility due to bidispersity requires fine particles to be segregated and located at the base. However, size segregation is not observed in large rock/debris avalanches. An assessment of the dynamic

scaling of the current lab-scale experiments and previous studies suggests that size segregation, and therefore the runout enhancing process, is scale-dependent and does not occur at the scale of natural rock/debris avalanches. The collisional flow regime enabled in the lab is not representative of the frictional regime of rock/debris avalanches. Therefore, bidispersity is unlikely to enhance the mobility of rock/debris avalanches by providing a more efficient basal shearing arrangement.

- This study highlights the dynamic scaling analysis, which must become a standard procedure in designing and interpreting analog granular avalanche experiments.

List of Abbreviations

R	horizontal runout of the front of the avalanche from the front of the material pre-release
R_{hCoM}	propagation of the center of mass on the horizontal plane
R_{CoM}	horizontal propagation distance of the center of mass
R_f	frontal runout on the horizontal plane
R_n	normalized frontal runout on the horizontal plane
R_{nCoM}	normalized propagation of the center of mass on the horizontal plane
ψ	proportion of fines
ψ_{CRf}	critical proportion of fines for maximum frontal runout
ψ_{CRcom}	critical proportion of fines for maximum propagation of the center of mass
V_f	frontal velocity
H	maximum fall height
H_{CoM}	vertical difference between the location of the center of mass in the box and in the final deposit
V	volume
h^*	$= V^{1/3}$
S_n	total spreading
S_f	frontal spreading
L	deposit length
Δ	size ratio between coarse and fine particles
V_{MAX}	maximum velocity in phase 2
N_{Sa}	Savage number
δ	typical particle diameter (m)
g	gravitational acceleration (ms^{-2})
T	avalanche thickness

Data Availability Statement

The processed data which support the described results, including video footage, digital element models of the deposits and measurements of runout, propagation, deposit geometry and spreading, are available on Zenodo at Makris et al. (2024). Photogrammetry was carried out using the commercially available software Agisoft PhotoScan Professional (Agisoft Photoscan, 2019). The Savage number values for natural events mentioned and discussed are from the catalog created by Li et al. (2021) and are presented in Appendix Table 2 of that publication.

Acknowledgments

This work was funded by the University of Plymouth through a Studentship (URS) to Symeon Makris. The authors would like to thank Amelia Dunn, Georgina White, Taylor Wood, and Jack Collingbridge, who carried out part of the experiments as part of their undergraduate dissertations for the University of Plymouth in 2020–2021. The authors would also like to thank the associate editor Dr Odin Marc and two anonymous reviewers for their constructive reviews.

References

AgiSoft PhotoScan Professional. (2019). Version 1.5.5 [Software]. Retrieved from <http://www.agisoft.com/downloads/installer/>

Ahmadipour, A., Qiu, T., & Sheikh, B. (2019). Investigation of basal friction effects on impact force from a granular sliding mass to a rigid obstruction. *Landslides*, 16(6), 1089–1105. <https://doi.org/10.1007/s10346-019-01156-0>

Ahmed, S. S., Martinez, A., Asce, A. M., Dejong, J. T., & Asce, F. (2023). Effect of gradation on the strength and stress-dilation behavior of coarse-grained soils in drained and undrained triaxial compression. *Journal of Geotechnical and Geoenvironmental Engineering*, 149(5), 1–21. <https://doi.org/10.1061/JGGEFK.GTENG-10972>

Baker, V. R. (1996). Hypotheses and geomorphological reasoning. In B. L. Rhoads, & C. E. Thorn (Eds.), *The scientific nature of geomorphology* (pp. 57–85). Wiley.

Banton, J., Villard, P., Jongmans, D., & Scavia, C. (2009). Two-dimensional discrete element models of debris avalanches: Parameterization and the reproducibility of experimental results. *Journal of Geophysical Research*, 114(F4), 1–15. <https://doi.org/10.1029/2008JF001161>

Bartali, R., Rodríguez Liñán, G. M., Torres-Cisneros, L. A., Pérez-Ángel, G., & Nahmad-Molinari, Y. (2020). Runout transition and clustering instability observed in binary-mixture avalanche deposits. *Granular Matter*, 22(2), 30. <https://doi.org/10.1007/s10035-019-0989-0>

Bartali, R., Sarocchi, D., & Nahmad-Molinari, Y. (2015). Stick-slip motion and high speed ejecta in granular avalanches detected through a multi-sensors flume. *Engineering Geology*, 195, 248–257. <https://doi.org/10.1016/j.enggeo.2015.06.019>

Bernard, B., Takarada, S., Andrade, S. D., & Dufresne, A. (2021). Terminology and strategy to describe large volcanic landslides and debris avalanches. In M. Roverato, A. Dufresne, & J. Procter (Eds.), *Volcanic debris avalanches: From collapse to hazard* (pp. 51–73). Springer Book Series Advances in Volcanology.

Bernard, K., Thouret, J. C., & van Wyk de Vries, B. (2017). Emplacement and transformations of volcanic debris avalanches—A case study at El Misti volcano, Peru. *Journal of Volcanology and Geothermal Research*, 340, 68–91. <https://doi.org/10.1016/j.jvolgeores.2017.04.009>

Bowman, E. T., Take, W. A., Rait, K. L., & Hann, C. (2012). Physical models of rock avalanche spreading behaviour with dynamic fragmentation. *Canadian Geotechnical Journal*, 49(4), 460–476. <https://doi.org/10.1139/T2012-007>

Breard, E. C. P., Dufek, J., Fullard, L., & Carrara, A. (2020). The basal friction coefficient of granular flows with and without excess pore pressure: Implications for pyroclastic density currents, water-rich debris flows, and rock and submarine avalanches. *Journal of Geophysical Research: Solid Earth*, 125(12), 1–22. <https://doi.org/10.1029/2020JB020203>

Cabrera, M., & Estrada, N. (2019). Granular column collapse: Analysis of grain-size effects. *Physical Review E—Statistical Physics, Plasmas, Fluids, and Related Interdisciplinary Topics*, 99, 1–7. <https://doi.org/10.1103/PhysRevE.99.012905>

Cabrera, M., & Estrada, N. (2021). Is the grain size distribution a key parameter for explaining the long runout of granular avalanches? *Journal of Geophysical Research: Solid Earth*, 126, 1–9. <https://doi.org/10.1029/2021JB022589>

Cagnoli, B., & Piersanti, A. (2015). Grain size and flow volume effects on granular flow mobility in numerical simulations: 3-D discrete element modeling of flows of angular rock fragments. *Journal of Geophysical Research: Solid Earth*, 3782–3803. <https://doi.org/10.1002/2015JB012608>

Cagnoli, B., & Romano, G. P. (2010). Effect of grain size on mobility of dry granular flows of angular rock fragments: An experimental determination. *Journal of Volcanology and Geothermal Research*, 193(1–2), 18–24. <https://doi.org/10.1016/j.jvolgeores.2010.03.003>

Cagnoli, B., & Romano, G. P. (2012). Effects of flow volume and grain size on mobility of dry granular flows of angular rock fragments: A functional relationship of scaling parameters. *Journal of Geophysical Research*, 117(B2), 1–13. <https://doi.org/10.1029/2011JB008926>

Campbell, C. S. (1990). Rapid granular flows. *Annual Review of Fluid Mechanics*, 22(1), 57–90. <https://doi.org/10.1146/annurev.fluid.22.1.57>

Crosta, G. B., De Blasio, F. V., De Caro, M., Volpi, G., Imposimato, S., & Roddeman, D. (2017). Modes of propagation and deposition of granular flows onto an erodible substrate: Experimental, analytical, and numerical study. *Landslides*, 14(1), 47–68. <https://doi.org/10.1007/s10346-016-0697-3>

Crosta, G. B., Frattini, P., & Fusi, N. (2007). Fragmentation in the Val Pola rock avalanche, Italian Alps. *Journal of Geophysical Research*, 112(F1), 1–23. <https://doi.org/10.1029/2005JF000455>

Cruden, D., & Hungr, O. (1986). The debris of the Frank Slide and theories of rockslide–avalanche mobility. *Canadian Journal of Earth Sciences*, 23(3), 425–432. <https://doi.org/10.1139/e86-044>

Davies, T. (1982). Spreading of rock avalanche debris by mechanical fluidization. *Rock Mechanics*, 24(1), 9–24. <https://doi.org/10.1007/bf01239474>

Davies, T., & McSaveney, M. (2012). Mobility of long-runout rock avalanches. In J. J. C. D. Stead, (Ed.), *Landslides: Types, mechanisms and modeling* (pp. 50–58).

Davies, T., & McSaveney, M. J. (1999). Runout of dry granular avalanches. *Canadian Geotechnical Journal*, 36(2), 313–320. <https://doi.org/10.1139/t98-108>

De Blasio, F. V. (2011). Introduction to the physics of landslides, introduction to the physics of landslides. <https://doi.org/10.1007/978-94-007-1122-8>

De Blasio, F. V., & Crosta, G. B. (2014). Simple physical model for the fragmentation of rock avalanches. *Acta Mechanica*, 225(1), 243–252. <https://doi.org/10.1007/s00707-013-0942-y>

Degaetano, M., Lacaze, L., & Phillips, J. C. (2013). The influence of localised size reorganisation on short-duration bidispersed granular flows. *European Physical Journal E: Soft Matter*, 36(4), 36. <https://doi.org/10.1140/epje/e2013-13036-9>

Denlinger, R. P., & Iverson, R. (2001). Flow of variably fluidized granular masses across three-dimensional terrain: 2. Numerical predictions and experimental tests. *Journal of Geophysical Research*, 106(B1), 537–552. <https://doi.org/10.1029/2000JB900329>

Drake, T. G. (1990). Structural features in granular flows. *Journal of Geophysical Research*, 95(B6), 8681–8696. <https://doi.org/10.1029/jb095ib06p08681>

Drake, T. G. (1991). Granular flow: Physical experiments and their implications for microstructural theories. *Journal of Fluid Mechanics*, 225, 121–152. <https://doi.org/10.1017/S0022112091001994>

Duan, Z., Wu, Y. B., Peng, J. B., & Xue, S. Z. (2022). Characteristics of sand avalanche motion and deposition influenced by proportion of fine particles. *Acta Geotechnica*, 18(3), 1353–1372. <https://doi.org/10.1007/s11440-022-01653-y>

Dufresne, A. (2009). *Influence of runout path material on rock and debris avalanche mobility: Field evidence and analogue modelling*. (Doctoral dissertation), University of Canterbury New Zealand 2009.

Dufresne, A. (2012). Granular flow experiments on the interaction with stationary runout path materials and comparison to rock avalanche events. *Earth Surface Processes and Landforms*, 37(14), 1527–1541. <https://doi.org/10.1002/esp.3296>

Dufresne, A., Bösmeier, A., & Prager, C. (2016). Sedimentology of rock avalanche deposits—Case study and review. *Earth-Science Reviews*, 163, 234–259. <https://doi.org/10.1016/j.earscirev.2016.10.002>

- Dufresne, A., & Dunning, S. (2017). Process dependence of grain size distributions in rock avalanche deposits. *Landslides*, 14(5), 1555–1563. <https://doi.org/10.1007/s10346-017-0806-y>
- Dufresne, A., Siebert, L., & Bernard, B. (2021). Distribution and geometric parameters of volcanic debris avalanche deposits. In *Volcanic debris avalanches* (pp. 75–90). Springer.
- Dunning, S. (2006). The grain-size distribution of rock avalanche deposits in valley-confined settings. *Italian Journal of Engineering Geology and Environment*, 1, 117–121. <https://doi.org/10.4408/IJEGE.2006-01.S-15>
- Dunning, S., & Armitage, P. J. (2011). The grain-size distribution of rock-avalanche deposits: Implications for natural dam stability. In *Natural and artificial rockslide dams* (pp. 479–498). Springer. <https://doi.org/10.1007/978-3-642-04764-0>
- Estrada, N. (2016). Effects of grain size distribution on the packing fraction and shear strength of frictionless disk packings. *Physical Review E—Statistical Physics, Plasmas, Fluids, and Related Interdisciplinary Topics*, 94(6), 062903. <https://doi.org/10.1103/PhysRevE.94.062903>
- Fan, X., Tian, S., & Zhang, Y. (2016). Mass-front velocity of dry granular flows influenced by the angle of the slope to the runout plane and particle size gradation. *Journal of Mountain Science*, 13(2), 234–245. <https://doi.org/10.1007/s11629-014-3396-3>
- Friedmann, S. J., Taberlet, N., & Losert, W. (2006). Rock-avalanche dynamics: Insights from granular physics experiments. *International Journal of Earth Sciences*, 95(5), 911–919. <https://doi.org/10.1007/s00531-006-0067-9>
- Glicken, H. (1996). Rockslide-debris avalanche of May 18, 1980, Mount St. Helens volcano, Washington. USGS Open File Report 96-677. *US Geological Survey*.
- Goujon, C., Dalloz-Dubrujeaud, B., & Thomas, N. (2007). Bidisperse granular avalanches on inclined planes: A rich variety of behaviors. *European Physical Journal E: Soft Matter*, 23(2), 199–215. <https://doi.org/10.1140/epje/i2006-10175-0>
- Gu, Y., Ozel, A., & Sundaresan, S. (2016). Rheology of granular materials with size distributions across dense-flow regimes. *Powder Technology*, 295, 322–329. <https://doi.org/10.1016/j.powtec.2016.03.035>
- Heim, A. (1932). *Bergsturz und menschenleben* (Vol. 77). Fretz & Wasmuth.
- Heller, V. (2011). Scale effects in physical hydraulic engineering models. *Journal of Hydraulic Research*, 49(3), 293–306. <https://doi.org/10.1080/00221686.2011.578914>
- Hergarten, S. (2024). Scaling between volume and runout of rock avalanches explained by a modified Voellmy rheology. *Earth Surface Dynamics*, 12(1), 219–229.
- Hewitt, K. (1998). Catastrophic landslides and their effects on the Upper Indus streams, Karakoram Himalaya, northern Pakistan. *Geomorphology*, 26(1–3), 47–80. [https://doi.org/10.1016/S0169-555X\(98\)00051-8](https://doi.org/10.1016/S0169-555X(98)00051-8)
- Hsü, K. J. (1975). Catastrophic debris streams (sturzstroms) generated by rockfalls. *Bulletin of the Geological Society of America*, 86(1), 129. [https://doi.org/10.1130/0016-7606\(1975\)86<129:CDSSGB>2.0.CO;2](https://doi.org/10.1130/0016-7606(1975)86<129:CDSSGB>2.0.CO;2)
- Hsü, K. J. (1978). Albert Heim: Observations on landslides and relevance to modern interpretations. In B. Voight (Ed.), *Rockslides and avalanches, 1. Natural phenomena* (pp. 71–93). Elsevier. <https://doi.org/10.1016/B978-0-444-41507-3.50009-X>
- Hsu, L., Dietrich, W. E., & Sklar, L. S. (2014). Mean and fluctuating basal forces generated by granular flows: Laboratory observations in a large vertically rotating drum. *Journal of Geophysical Research: Earth Surface*, 119(6), 1283–1309. <https://doi.org/10.1002/2013JF003078>
- Hu, Y. X., Li, H. B., Lu, G. D., Fan, G., & Zhou, J. W. (2021). Influence of size gradation on particle separation and the motion behaviors of debris avalanches. *Landslides*, 18(5), 1845–1858. <https://doi.org/10.1007/s10346-020-01596-z>
- Hu, Y. X., Li, H. B., Qi, S. C., Fan, G., & Zhou, J. W. (2020). Granular effects on depositional processes of debris avalanches. *KSCE Journal of Civil Engineering*, 24(4), 1116–1127. <https://doi.org/10.1007/s12205-020-1555-3>
- Hughes, A., Kendrick, J. E., Salas, G., Wallace, P. A., Legros, F., Di Toro, G., & Lavallée, Y. (2020). Shear localisation, strain partitioning and frictional melting in a debris avalanche generated by volcanic flank collapse. *Journal of Structural Geology*, 140, 104132. <https://doi.org/10.1016/j.jsg.2020.104132>
- Hungr, O. (2002). Rock avalanche occurrence, process and modelling. In S. Evans, G. Scarascia-Mugnozza, A. Strom, & R. Hermanns (Eds.), *Landslides from massive rock slope failure* (pp. 285–304). Springer.
- Hungr, O., & Evans, S. (2004). Entrainment of debris in rock avalanches: An analysis of a long run-out mechanism. *Bulletin of the Geological Society of America*, 116(9), 1240–1252. <https://doi.org/10.1130/B25362.1>
- Hungr, O., Leroueil, S., & Picarelli, L. (2014). The Varnes classification of landslide types, an update. *Landslides*, 11(2), 167–194. <https://doi.org/10.1007/s10346-013-0436-y>
- Iverson, R. (1997). The physics of debris flows. *Reviews of Geophysics*, 35(3), 245–296. <https://doi.org/10.1029/97RG00426>
- Iverson, R. (2015). Scaling and design of landslide and debris-flow experiments. *Geomorphology*, 244, 9–20. <https://doi.org/10.1016/j.geomorph.2015.02.033>
- Iverson, R., & Denlinger, R. P. (2001). Flow of variably fluidized granular masses across three-dimensional terrain: 1. Coulomb mixture theory. *Journal of Geophysical Research*, 106(B1), 537–552. <https://doi.org/10.1029/2000JB900329>
- Iverson, R., Logan, M., & Denlinger, R. P. (2004). Granular avalanches across irregular three-dimensional terrain: 2. Experimental tests. *Journal of Geophysical Research*, 109(F1), 1–16. <https://doi.org/10.1029/2003jf000084>
- Iverson, R. M., & Vallance, J. W. (2001). New views of granular mass flows. *Geology*, 29(2), 115–118. [https://doi.org/10.1130/0091-7613\(2001\)029<0115:NVOGMF>2.0.CO;2](https://doi.org/10.1130/0091-7613(2001)029<0115:NVOGMF>2.0.CO;2)
- Jiang, Y. J., & Zhao, Y. (2015). Experimental investigation of dry granular flow impact via both normal and tangential force measurements. *Géotechnique Letters*, 5(1), 33–38. <https://doi.org/10.1680/geolett.15.00003>
- Johnson, B. C., Campbell, C. S., & Melosh, J. H. (2016). The reduction of friction in long runout landslides as an emergent phenomenon. *Journal of Geophysical Research: Earth Surface*, 300–316. <https://doi.org/10.1002/2013JF002871>
- Knapp, S., & Krautblatter, M. (2020). Conceptual framework of energy dissipation during disintegration in rock avalanches. *Frontiers in Earth Science*, 8, 1–9. <https://doi.org/10.3389/feart.2020.00263>
- Kokelaar, B. P., Graham, R. L., Gray, J. M. N. T., & Vallance, J. W. (2014). Fine-grained linings of leveed channels facilitate runout of granular flows. *Earth and Planetary Science Letters*, 385, 172–180. <https://doi.org/10.1016/j.epsl.2013.10.043>
- Lai, Z., Vallejo, L. E., Zhou, W., Ma, G., Espitia, J. M., Caicedo, B., & Chang, X. (2017). Collapse of granular columns with fractal particle size distribution: Implications for understanding the role of small particles in granular flows. *Geophysical Research Letters*, 44(24), 12181–12189. <https://doi.org/10.1002/2017GL075689>
- Legros, F. (2002). The mobility of long-runout landslides. *Engineering Geology*, 63(3–4), 301–331. [https://doi.org/10.1016/S0013-7952\(01\)00090-4](https://doi.org/10.1016/S0013-7952(01)00090-4)
- Li, G., Liu, Y.-J., Dano, C., & Hicher, P.-Y. (2015). Grading-dependent behavior of granular materials: From discrete to continuous modeling. *Journal of Engineering Mechanics*, 141(6). [https://doi.org/10.1061/\(ASCE\)EM.1943-7889.0000866](https://doi.org/10.1061/(ASCE)EM.1943-7889.0000866)
- Li, K., Wang, Y. F., Lin, Q. W., Cheng, Q. G., & Wu, Y. (2021). Experiments on granular flow behavior and deposit characteristics: Implications for rock avalanche kinematics [Dataset]. *Landslides*, 18(5), 1779–1799. <https://doi.org/10.1007/s10346-020-01607-z>

- Linares-Guerrero, E., Goujon, C., & Zenit, R. (2007). Increased mobility of bidisperse granular avalanches. *Journal of Fluid Mechanics*, 593, 475–504. <https://doi.org/10.1017/S0022112007008932>
- Makris, S., Manzella, I., Cole, P., & Roverato, M. (2020). Grain size distribution and sedimentology in volcanic mass-wasting flows: Implications for propagation and mobility. *International Journal of Earth Sciences*, 109(8), 2679–2695. <https://doi.org/10.1007/s00531-020-01907-8>
- Makris, S., Manzella, I., & Sgarabotto, A. (2024). Scale-dependent processes and runoff in bidisperse granular flows: Insights from laboratory experiments and implications for rock/debris avalanches [DATA REPOSITORY]. *Zenodo*. <https://doi.org/10.5281/zenodo.10814560>
- Makris, S., Roverato, M., Dávila-harris, P., Cole, P., & Manzella, I. (2023). Distributed stress fluidisation: Insights into the propagation mechanisms of the Abona volcanic debris avalanche (Tenerife) through a novel method for indurated deposit sedimentological analysis. *Frontiers in Earth Science*, 11, 1–22. <https://doi.org/10.3389/feart.2023.1177507>
- Makris, S., Roverato, M., Lomoschitz, A., Cole, P., Manzella, I., & Canaria, G. (2023). The propagation and emplacement mechanisms of the Tenteniguada volcanic debris avalanche (Gran Canaria): Field evidence for brittle fault-accommodated spreading. *Journal of Volcanology and Geothermal Research*, 435, 107773. <https://doi.org/10.1016/j.jvolgeores.2023.107773>
- Mangeny, A., Roche, O., Hungr, O., Mangold, N., Faccanoni, G., & Lucas, A. (2019). Erosion and mobility in granular collapse over sloping beds. *Journal of Geophysical Research*, 115(F3), 1–21. <https://doi.org/10.1029/2019JF001462>
- Manzella, I., Einstein, H. H., & Grasselli, G. (2013). DEM and FEM/DEM modelling of granular flows to investigate large debris avalanche propagation. In *Landslide science and practice: Spatial analysis and modelling* (pp. 247–253). <https://doi.org/10.1007/978-3-642-31310-3-33>
- Manzella, I., & Labiouse, V. (2009). Flow experiments with gravel and blocks at small scale to investigate parameters and mechanisms involved in rock avalanches. *Engineering Geology*, 109(1–2), 146–158. <https://doi.org/10.1016/j.enggeo.2008.11.006>
- Manzella, I., & Labiouse, V. (2013). Empirical and analytical analyses of laboratory granular flows to investigate rock avalanche propagation. *Landslides*, 10(1), 23–36. <https://doi.org/10.1007/s10346-011-0313-5>
- Marc, O., Turowski, J. M., & Meunier, P. (2021). Controls on the grain size distribution of landslides in Taiwan: The influence of drop height, scar depth and bedrock strength. *Earth Surface Dynamics*, 9(4), 995–1011. <https://doi.org/10.5194/esurf-9-995-2021>
- McSaveney, M. J. (1978). Sherman glacier rock avalanche, Alaska, U.S.A. In *Developments in geotechnical engineering*. Elsevier Scientific Publishing Company. <https://doi.org/10.1016/B978-0-444-41507-3.50014-3>
- McSaveney, M. J., & Davies, T. (2002). Rapid rock-mass flow with dynamic fragmentation: Inferences from the morphology and internal structure of rockslides and rock avalanches. In S. Evans, G. Scarascia Mugnozza, A. Strom, & R. Hermanns (Eds.), *Landslides from massive rock slope failure* (pp. 285–304). Springer.
- McSaveney, M. J., Davies, T., & Hodgson, K. A. (2000). A contrast in deposit style and process between large and small rock avalanches. In *Proceedings of the 8th international symposium on landslides* (pp. 26–30).
- McSaveney, M. J., & Davies, T. R. (1999). The Falling Mountain rock avalanche of 1929. *Arthur's Pass National Park. Institute of Geological and Nuclear Sciences Science Report*.
- Middleton, G. V. (1976). Subaqueous sediment transport and deposition by sediment gravity flows. *Marine sediment transport and environment management*, 197–218.
- Moro, F., Faug, T., Bellot, H., & Ousset, F. (2010). Large mobility of dry snow avalanches: Insights from small-scale laboratory tests on granular avalanches of bidisperse materials. *Cold Regions Science and Technology*, 62(1), 55–66. <https://doi.org/10.1016/j.coldregions.2010.02.011>
- Oda, M., & Kazama, H. (1998). Microstructure of shear bands and its relation to the mechanisms of dilatancy and failure of dense granular soils. *Géotechnique*, 48(4), 465–481. <https://doi.org/10.1680/geot.1998.48.4.465>
- Paguican, E. M., Roverato, M., & Yoshida, H. (2021). Volcanic debris avalanche transport and emplacement mechanisms. In M. Roverato, A. Dufresne, & J. Procter (Eds.), *Volcanic debris avalanches: From collapse to hazard* (pp. 143–173). Springer Book Series Advances in Volcanology. https://doi.org/10.1007/978-3-030-57411-6_7
- Perinotto, H., Schneider, J. L., Bachèlery, P., Le Bourdonnec, F. X., Famin, V., & Michon, L. (2015). The extreme mobility of debris avalanches: A new model of transport mechanism. *Journal of Geophysical Research: Solid Earth*, 120(12), 8110–8119. <https://doi.org/10.1002/2015JB011994>
- Phillips, J. C., Hogg, A. J., Kerswell, R. R., & Thomas, N. H. (2006). Enhanced mobility of granular mixtures of fine and coarse particles. *Earth and Planetary Science Letters*, 246(3–4), 466–480. <https://doi.org/10.1016/j.epsl.2006.04.007>
- Polanía, O., Cabrera, M., Renouf, M., Azéma, E., & Estrada, N. (2023). Grain size distribution does not affect the residual shear strength of granular materials: An experimental proof. *Physical Review E—Statistical Physics, Plasmas, Fluids, and Related Interdisciplinary Topics*, 107(5), 052901. <https://doi.org/10.1103/PhysRevE.107.L052901>
- Pollet, N., & Schneider, J. L. M. (2004). Dynamic disintegration processes accompanying transport of the Holocene Flims sturzstrom (Swiss Alps). *Earth and Planetary Science Letters*, 221(1–4), 433–448. [https://doi.org/10.1016/S0012-821X\(04\)00071-8](https://doi.org/10.1016/S0012-821X(04)00071-8)
- Pudasaini, S. P., & Hutter, K. (2007). *Avalanche dynamics: Dynamics of rapid flows of dense granular avalanches*. Springer Science & Business Media.
- Pudasaini, S. P., Wang, Y., & Hutter, K. (2005). Rapid motions of free-surface avalanches down curved and twisted channels and their numerical simulation. *Philosophical Transactions of the Royal Society A: Mathematical, Physical and Engineering Sciences*, 363(1832), 1551–1571. <https://doi.org/10.1098/rsta.2005.1595>
- Rait, K. L., & Bowman, E. T. (2016). Influences of strain rate and shear rate on the propagation of large scale rock avalanches. In *Landslides and engineered slopes. Experience, theory and practice* (Vol. 3, pp. 1707–1714). <https://doi.org/10.1201/b21520-212>
- Reubi, O., & Hernandez, J. (2000). Volcanic debris avalanche deposits of the upper Maronne valley (Cantal Volcano, France): Evidence for contrasted formation and transport mechanisms. *Journal of Volcanology and Geothermal Research*, 102(3–4), 271–286. [https://doi.org/10.1016/S0377-0273\(00\)00191-8](https://doi.org/10.1016/S0377-0273(00)00191-8)
- Reubi, O., Ross, P. S., & White, J. D. L. (2005). Debris avalanche deposits associated with large igneous province volcanism: An example from the Mawson Formation, central Allan Hills, Antarctica. *Bulletin of the Geological Society of America*, 117(11), 1615–1628. <https://doi.org/10.1130/B25766.1>
- Roche, O., Gilbertson, M. A., Phillips, J. C., & Sparks, R. S. J. (2006). The influence of particle size on the flow of initially fluidised powders. *Powder Technology*, 166(3), 167–174. <https://doi.org/10.1016/j.powtec.2006.05.010>
- Roche, O., van den Wildenberg, S., Valance, A., Delannay, R., Mangeny, A., Corna, L., & Latchimy, T. (2021). Experimental assessment of the effective friction at the base of granular chute flows on a smooth incline. *Physical Review E—Statistical Physics, Plasmas, Fluids, and Related Interdisciplinary Topics*, 103(4), 042905. <https://doi.org/10.1103/PhysRevE.103.042905>
- Rognon, P. G., Roux, J.-N., Naaim, M., & Chevoir, F. (2007). Dense flows of bidisperse assemblies of disks down an inclined plane. *Physics of Fluids*, 19(5), 58101. <https://doi.org/10.1063/1.2722242>
- Roverato, M., Cronin, S., Procter, J., & Capra, L. (2015). Textural features as indicators of debris avalanche transport and emplacement, Taranaki volcano. *Bulletin of the Geological Society of America*, 127(1–2), 3–18. <https://doi.org/10.1130/B30946.1>

- Roverato, M., Dufresne, A., & Procter, J. (2021). Volcanic debris avalanches: From collapse to hazard.
- Sanvitale, N., & Bowman, E. T. (2016). Using PIV to measure granular temperature in saturated unsteady polydisperse granular flows. *Granular Matter*, 18(3), 1–12. <https://doi.org/10.1007/s10035-016-0620-6>
- Savage, S. B. (1984). The mechanics of rapid granular flows. *Advances in Applied Mechanics*, 24, 289–366. [https://doi.org/10.1016/s0065-2156\(08\)70047-4](https://doi.org/10.1016/s0065-2156(08)70047-4)
- Savage, S. B., & Hutter, K. (1989). The motion of a finite mass of granular material down a rough incline. *Journal of Fluid Mechanics*, 199, 177–215. <https://doi.org/10.1017/s0022112089000340>
- Savage, S. B., & Lun, C. K. K. (1988). Particle size segregation in inclined chute flow of dry cohesionless granular solids. *Journal of Fluid Mechanics*, 189, 311–335. <https://doi.org/10.1017/S002211208800103X>
- Schilirò, L., Esposito, C., De Blasio, F. V., & Scarascia Mugnozza, G. (2019). Sediment texture in rock avalanche deposits: Insights from field and experimental observations. *Landslides*, 16(9), 1629–1643. <https://doi.org/10.1007/s10346-019-01210-x>
- Schneider, J. L., & Fisher, R. V. (1998). Transport and emplacement mechanisms of large volcanic debris avalanches: Evidence from the northwest sector of Cantal Volcano (France). *Journal of Volcanology and Geothermal Research*, 83(1–2), 141–165. [https://doi.org/10.1016/S0377-0273\(98\)00016-X](https://doi.org/10.1016/S0377-0273(98)00016-X)
- Scott, K., Macias, J. L., Naranjo, J. A., Rodriguez, S., & McGeehin, J. P. (2001). *Catastrophic debris flows transformed from landslides in volcanic terrains: Mobility, hazard assessment, and mitigation strategies*. US Geological Survey Professional Paper.
- Scott, K., Vallance, J. W., & Pringle, P. T. (1995). Sedimentology, behavior, and hazards of debris flows at Mount Rainier, Washington. *U. S. Geological Survey Professional Paper*, 1547, 1–66. <https://doi.org/10.1016/j.radonc.2016.01.020>
- Shea, T., & van Wyk de Vries, B. (2008). Structural analysis and analogue modeling of the kinematics and dynamics of rockslide avalanches. *Geosphere*, 4(1), 657–686. <https://doi.org/10.1130/GES00131>
- Shreve, R. L. (1966). Sherman landslide, Alaska. *Science*, 154(3757), 1639–1643. <https://doi.org/10.1126/science.154.3757.1639>
- Silbert, L. E., Ertas, D., Grest, G. S., Halsey, T. C., Levine, D., & Plimpton, S. J. (2001). Granular flow down an inclined plane: Bagnold scaling and rheology. *Physical Review E—Statistical Physics, Plasmas, Fluids, and Related Interdisciplinary Topics*, 64(5), 14. <https://doi.org/10.1103/PhysRevE.64.051302>
- Thompson, N., Bennett, M. R., & Petford, N. (2009). Analyses on granular mass movement mechanics and deformation with distinct element numerical modeling: Implications for large-scale rock and debris avalanches. *Acta Geotechnica*, 4, 233–247. <https://doi.org/10.1007/s11440-009-0093-4>
- Tripathi, A., & Khakhar, D. V. (2011). Rheology of binary granular mixtures in the dense flow regime. *Physics of Fluids*, 23(11). <https://doi.org/10.1063/1.3653276>
- Ui, T. (1983). Volcanic dry avalanche deposits—Identification and comparison with nonvolcanic debris stream deposits. *Journal of Volcanology and Geothermal Research*, 18(1–4), 135–150. [https://doi.org/10.1016/0377-0273\(83\)90006-9](https://doi.org/10.1016/0377-0273(83)90006-9)
- Valentino, R., Barla, G., & Montrasio, L. (2008). Experimental analysis and micromechanical modelling of dry Granular flow and impacts in laboratory flume tests. *Rock Mechanics and Rock Engineering*, 41(1), 153–177. <https://doi.org/10.1007/s00603-006-0126-3>
- Vallance, J. W. (2000). Lahars. In *The encyclopedia of volcanoes* (pp. 601–616).
- Vallance, J. W., & Iverson, R. (2015). Lahars and their deposits. In *The encyclopedia of volcanoes* (2nd ed.). Elsevier. <https://doi.org/10.1016/b978-0-12-385938-9.00037-7>
- Van Gassen, W., & Cruden, D. M. (1989). Momentum transfer and friction in the debris of rock avalanches. <https://doi.org/10.1139/t89-075>
- Voight, B. (1978). *Rockslides and avalanches. I. Natural phenomena*. Elsevier.
- Voight, B., Janda, R. J., Glicken, H., & Douglass, P. M. (1983). Nature and mechanics of the Mount St Helens rockslide-avalanche of 18 May 1980. *Géotechnique*, 33(3), 243–273. <https://doi.org/10.1680/geot.1983.33.3.243>
- Walton, O. R. (1993). Numerical simulation of inclined chute flows of monodisperse, inelastic, frictional spheres. *Mechanics of Materials*, 16(1–2), 239–247. [https://doi.org/10.1016/0167-6636\(93\)90048-v](https://doi.org/10.1016/0167-6636(93)90048-v)
- Wang, Y. F., Cheng, Q. G., Shi, A. W., Yuan, Y. Q., Yin, B. M., & Qiu, Y. H. (2019). Sedimentary deformation structures in the Nyixoi Chongco rock avalanche: Implications on rock avalanche transport mechanisms. *Landslides*, 16(3), 523–532. <https://doi.org/10.1007/s10346-018-1117-7>
- Yang, J., & Luo, X. D. (2018). The critical state friction angle of granular materials: Does it depend on grading? *Acta Geotechnica*, 13(3), 535–547. <https://doi.org/10.1007/s11440-017-0581-x>
- Yang, Q., Cai, F., Ugai, K., Yamada, M., Su, Z., Ahmed, A., et al. (2011). Some factors affecting mass-front velocity of rapid dry granular flows in a large flume. *Engineering Geology*, 122(3–4), 249–260. <https://doi.org/10.1016/j.enggeo.2011.06.006>
- Yang, Q., Su, Z., Cai, F., & Ugai, K. (2015). Enhanced mobility of polydisperse granular flows in a small flume. *Geoenvironmental Disasters*, 2(1), 12. <https://doi.org/10.1186/s40677-015-0019-4>
- Zhu, Y., Nie, Z., Gong, J., Zou, J., Zhao, L., & Li, L. (2020). An analysis of the effects of the size ratio and fines content on the shear behaviors of binary mixtures using DEM. *Computers and Geotechnics*, 118, 103353. <https://doi.org/10.1016/j.compgeo.2019.103353>